REVIEW

The flexural response of RC beams strengthened by EB/NSM techniques using FRP and metal materials: a state-of-the-art review

F. A. Megahed[1] · M. H. Seleem[1] · A. A. M. Badawy[1] · I. A. Sharaky[1,2]

Abstract
Reinforced concrete (RC) beams strengthened in flexure using externally bonded (EB) or near-surface mounted (NSM) fiber-Reinforced Polymers (FRP) and metals have gained considerable interest over the last few decades. As few of the previous review papers concerned with NSM elements or both EB and NSM methods so this paper aimed to review the previous research that handled the behavior of RC beams strengthened by NSM and EB techniques, compared their advantages and disadvantages and reported the future recommendations. Moreover, the review focused on the effect of strengthening materials (metallic and FRP materials), strengthening method, strengthening elements characteristics (shape and area), and any other factors affecting the performance of the strengthened RC beams in each technique. The review demonstrated that the strengthening element's failure mode significantly affects the RC beams' load-carrying capacity strengthened by EB or NSM. Moreover, the type of FRP materials and the end anchorage significantly affect the load efficiency of the strengthened RC beams depending on the type of failure mode.

Keywords Fiber-reinforced polymer (FRP) · Externally bonded (EB) · Near-surface mounted (NSM) · Load capacity · Failure modes · End anchorage

Introduction

The deterioration of reinforced concrete (RC) structures leading to a loss in strength became a communal problem that could be attributed to many causes, from corrosion and chloride attack to inadequate design. Increasing required load specifications or live loads might also be another issue.

Using fiber-reinforced polymers (FRP) composites as strengthening reinforcement has been proven to be an effective and efficient solution [1]. The FRP composites involve continuous fibers embedded in a polymeric matrix that link the substrate and fibers, transmitting stress from one to the other [2]. The bonded FRP materials may be carbon fiber-reinforced polymer (CFRP) or glass fiber-reinforced polymer (GFRP) plates/bars [3]. The benefits of this material are its high strength-to-weight ratio, corrosion resistance, low thermal conductivity, and application versatility [4].

To overcome the adverse effects of these conditions, it is necessary to strengthen the RC beams with suitable tactics. Various methods were proposed to reinforce existing RC structures. These methods include shotcrete for rehabilitation, externally bonded (EB) [5], near-surface mounted (NSM) [6], and textile-reinforced mortar (TRM) [7]. The EB technique upgraded the RC elements by bonding steel or FRP plates/bars to their tension faces [8]. In the NSM strengthening technique, slits were formed in the concrete cover, and the reinforcement was embedded into it with groove filler (epoxy or cement mortar). The NSM efficiency made it an effective technique to upgrade the RC elements [9]. In the first appearance of the NSM technique, steel bars embedded in cement mortar were the basic strengthening concept. Eventually, shotcrete was used to cover the exterior

✉ F. A. Megahed
fatma.m021@eng.zu.edu.eg

M. H. Seleem
mhseleem1963@gmail.com

A. A. M. Badawy
aam_badawy@yahoo.com

I. A. Sharaky
ibm_attia@zu.edu.eg

1 Materials Engineering Department, Faculty of Engineering, Zagazig University, Zagazig 44519, Egypt

2 Civil Engineering Department, College of Engineering, Taif University, P.O. Box 11099, 21944 Taif, Saudi Arabia

of the bars. However, these procedures failed to develop a good bond between concrete and steel. Also, casting concrete around large strengthening structures was not practical. Recently, several studies dealt with the strengthening of RC members by adopting the NSM technique using the CFRP bars [6], CFRP strips [10], CFRP laminates [11], and GFRP bars [12, 13] were performed. Consequently, this review article gives insight into the current developments in strengthening RC beams using NSM and EB techniques and future work recommendations.

Numerous review papers reported several data about the behavior of RC beams strengthened with the EB technique [14–36]. However, few reviews concerned NSM elements [37–42] or both EB and NSM methods [43–46]. All the previous review papers treated with certain factors affecting the EB and the NSM techniques. Therefore, this paper aims to collect and review the studies available up to date regarding the strengthening of the RC beams with the EB method and NSM reinforcement. The review included information related to the strengthening materials (metallic and FRP composites), epoxy properties, factors affecting the two techniques, ductility analysis, and the failure modes of the strengthened elements in each technique. The paper also highlighted the gap in the EB and NSM strengthening methods and introduces future recommendations to enhance

the two approaches. Figure 1 shows the flowchart describing the paper layout.

Flexural behavior of the strengthened RC beams with EB technique

Table 1 reviews a sample of the studies that used the EB technique to enhance the flexural capacity of the RC elements. The attained load that yields the flexural steel reinforcement (P_y), deflection level when the steel yields (δy), load-carrying capacity (P_u), and the percentage increase of P_u over that of the control beam (CB) ($P_u\%$), deflection at ultimate and failure loads (δ_u and δ_f, respectively) are illustrated in the table.

Summary of the existing studies related to the EB technique

RC beams strengthened with EB-FRP sheets or laminates

Various studies investigated the utilization of EB CFRP plates or sheets to increase RC beams' strength [5, 47, 53, 55–75]. The flexural strength of continuous beams strengthened externally with CFRP sheets or plates was evaluated

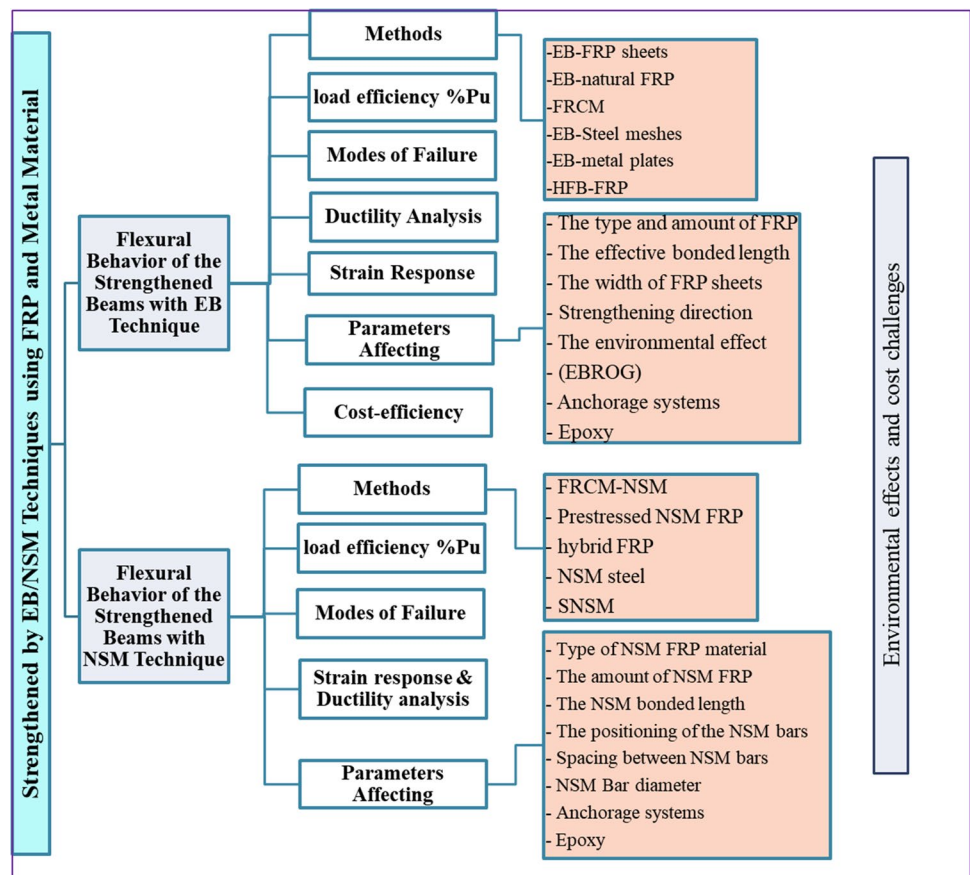**Fig. 1** Flowchart describing the paper layout

Table 1 Studies on RC beams strengthened with EB technique

Author	Method and epoxy	Sample parameters	P_u (%)	Deflection (mm)			Failure mode	Ductility Index	
				δy (mm)	δu (mm)	δf (mm)		$\mu_{\Delta ult}$ ($\delta u/\delta y$)	% Dec
Salama et al. [47]	(Bottom or side-bonded) of the CFRP sheets and V-wrap 700 epoxy adhesive	Bottom Sheet, 1 Ply	62.0	8.0	18.3	18.4	SC-F	2.28	16.8
		Bottom Sheet, 2 Plies	92.0	8.7	15.3	15.3	S-F	1.77	35.6
		Side Sheets, 1 Ply	66.0	7.0	14.7	15.2	SC-F	2.09	23.8
		Side Sheets, 2 Plies	84.4	8.8	12.9	13.1	SC-F	1.68	38.8
		SSB, 1 Ply 50 mm	39.7	7.6	14.4	14.8	SC-F	1.89	31.1
		SSB, 1 Ply 150 mm	87.2	9.8	16.5	16.8	SC-F	1.47	46.4
		SSB, 2 Plies 50 mm	58.8	7.6	13.1	13.3	S-F	1.69	38.4
		SSB, 2 Plies 150 mm	93.4	8.9	15.1	15.9	SC-F	1.74	36.7
Chen et al. [48]	Two types of NFRP: flax and jute	2-layer CFRP	32	11.61	28.13		S-F+Fr	2.42	21
		2-layers—jute fabric	17	8.98	18.33		Fr	2.04	33
		3-layers -jute fabric	0	9.83	12.88		Fr	1.31	57
		4-layers-bidirectional flax	18	9.78	26.15		Fr	2.67	13
		8-layer unidirectional flax fabric	40	11.61	35.01		S-F+Fr	3.02	2
Huang et al. [49]	FFRP	2Ø8 mm- 4 layers	67	2.7	17.2	19.23	SFr	6.5	+160
		2Ø8 mm- 6 layers	105	4.0	23.4	24.74		5.9	+136
		2Ø12 mm- 4 layers	15	5.2	19.3	22.13		3.7	+48
		2Ø12 mm- 6 layers	21	5.4	21.9	22.34		4.0	+60
	FFRP applies 80% of Py of the CB	2Ø8 mm- 4 layers	71	2.4	16.9	17.90		7.1	+180
		2Ø8 mm- 6 layers	113	3.3	22.8	23.89		7.0	+180
Abdallaa et al. [50]	3 mm thick AA-plates oriented at 90° and 45°, Sika	oriented at 90°	19	5.74	5.74	5.75	SH	1.00	–
		oriented at 45°	39	6.29	8.23	9.57	SH	1.16	–

Table 1 (continued)

Author	Method and epoxy	Sample parameters	P_u (%)	Deflection (mm)			Failure mode	Ductility Index	
				δy (mm)	δu (mm)	δf (mm)		$μ_{Δult}$ (δu/δy)	% Dec
Rasheed et al. [51]	2 mm thick AA plates or 3 mm thick AA plates, with single and double-end CFRP sheet U-wraps by Sikadur-330 with SikaWrap-300C for CFRP sheet	2 mm AA Plates	15.3	7.13	28.19	34.75	IC	3.95	+ 13
		2 mm AA Plates	13.3	6.23	22.85	27.08	IC	3.67	+ 5
		2 mm AA Plates 1U-wraps Anchorage	24.8	6.15	20.44	34.53	IC	3.32	5
		2 mm AA Plates 2U-wraps Anchorage	21.4	7.18	48.15	48.15	IC	6.71	+ 90
		3 mm AA Plates	40.0	7.20	25.16	25.92	IC	3.49	0
		3 mm AA Plates 1U-wraps Anchorage	29.2	6.65	21.37	29.55	IC	3.21	9
		3 mm AA Plates 2U-wraps Anchorage	26.2	6.82	24.71	37.56	IC	3.62	+ 4
		3 mm AA Plates 2U-wraps Anchorage	26.4	7.54	23.11	30.57	IC	3.06	13
Hawileh et al. [52]	HSF width = 40,70,100,120 mm and Sikadur 30LP	1-layer med-density steel sheet	44.0	10.3	17.82	18.3	SC-F	1.73	13
		2-layers of med-density steel sheet	56.4	9.32	11.51	12.2	SC-F	1.23	38
		1-layer of high-density steel sheet	47.8	11.2	15.80	16.15	SC-F	1.41	29
		2-layers of high-density steel sheet	62	8.62	12.10	12.1	SC-F	1.40	30
		2-layers of high-density steel sheet	41.6	9.31	14.25	14.3	SC-F	1.53	23
		2-layers of med-density steel sheet	29.3	10.5	12.85	12.14	SC-F	1.22	39
		2-layers of med-density steel sheet	33.4	10.4	12.18	13.12	SC-F	1.17	41
Hawileh et al. [53]		1 layer of CFRP	57.3	8.59	18.55	19.39	SC-F	2.16	38
		1 layer of GFRP	30.8	7.40	20.69	23.21	SC-F	2.80	20
		1-layer GFRP / CFRP	83.0	7.80	15.75	20.10	SC-F	2.02	42
		1 GFRP/ CFRP/ GFRP	98.0	8.86	14.11	26.90	S-C	1.59	55
Zhou et al. [54]	epoxy resin (Good-bond JN-C3P)	CFRP sheets	9.47		25.48		IC		–
		1 CFRP sheets + hybrid anchored	24.21		56.56		Fr		–
		2 layers CFRP sheets + 2 plies hybrid anchored	45.26		51.76		SC-F		–

Table 1 (continued)

Author	Method and epoxy	Sample parameters	P_u (%)	Deflection (mm)			Failure mode	Ductility Index	
				δy (mm)	δu (mm)	δf (mm)		$\mu_{\Delta ult}$ ($\delta u/\delta y$)	% Dec
Hosen et al. [55]	0.005main steel reinforcing ratios and Sikadur-330	pre-cracking load (0%)	154		–		S-F		48
		Pre-cracking load 60%	161		–				47
		Pre-cracking load 80%	155		–				49
	0.0071 main steel reinforcing ratios and Sikadur-330	pre-cracking load (0%)	99		–		SC-F		31
		Pre-cracking load 60%	102		–		SC-F		31
		Pre-cracking load 80%	100		–		S-F		30
Nader et al. [56]	EBROG End anchorage	0 prestressing strain	38.3		11.78	27.75	S-F	2.4	31
		20% prestress strain	48.1		13.52	23.22	S-F	1.7	51
		30% prestress strain	16.2		–	14.02	SC-F	–	–
		20% prestress strain	62.4		12.67	29.67	S-F	2.3	34
		30% prestress strain	66.1		13.27	28.67	S-F	2.2	37

by Abdallah et al. [5]. The results indicated that continuous beams had positive (sagging) and negative (hogging) bending moment regions, proving a 59.1% and 49.8% load improvement for the yield and ultimate loads due to the EB-CFRP composites application. Moreover, the weightier CFRP sheet improved strength more than multiple sheet layer additions. Consequently, Dong et al. [57] found that flexural strengthening of RC beams with EB CFRP sheets resulted in a 41–125% increase in P_u compared to its CB capacity. Conversely, Al-Tamimi et al. [58] implemented a single layer of U-wrapping sheets and two layers of U-wrap sheets with perpendicular fiber orientation (one layer in longitudinal and the other in transverse direction) to anchorage the CFRP palates. It was disclosed that, as the CFRP plates were implemented with or without end anchorage, the beams' load efficiency (P_u%) increased by 5%-80%. Furthermore, Ahmedet al. [59] used CFRP laminates with single, double, and triple layers to strengthen RC beams with one U-shaped strip and two W-shaped edge strips. The results guaranteed that the flexural stiffness, yield load, and ultimate load were increased with increasing the CFRP laminate layers. Also, the maximum gain in the flexural strength was more significant in beams with low FRP reinforcement ratios having end anchorage. Moreover, the tensile force was taken up by FRP systems when the steel bars yielded and tended to increase the beam capacity. In addition, El-Sayed et al. [60]

tested two beams under static flexural loading to determine the ultimate capacity of the beams. One of the two beams was strengthened with CFRP plates, and the other was unstrengthened. The beam experienced an increase of about 77% in the P_u due to the inclusion of CFRP reinforcement with about 36–40% reduction in mid-span deflection.

Conversely, Yin and Wu [61] tested a short beam without EB FRP sheets reinforced with different volume fractions of steel-fibers (0–1.0%) to verify the enhancement of concrete toughness. They tested a series of FRP beams strengthened with the same steel-fiber volume fractions to show how the enhanced concrete toughness affects the FRP strengthening performance. They found minimal changes in the tensile strength with increasing steel fiber volume fraction. In contrast, notable increases were recorded in the debonding initiation, peak loads, and FRP stress transfer length. Alternatively, Aliet al. [62] strengthened the continuously RC beams by bonding CFRP and GRFP sheets and tested them in bending. Compared to the CB, the ultimate load of the beam strengthened by CFRP sheets increased by 16.7 and 26.6%, while those strengthened by GFRP sheets increased by 7.2%.

As well-known aramid fiber-reinforced polymer (AFRP) is a highly effective synthetic fiber in textiles and composites. This type of fiber has many advantages, such as great strength, high elasticity, and heat resistance, with a density

40% lower than GFRP but at a somewhat higher cost [63]. Zhang and Wu [64] studied how saltwater immersion could influence the twenty-two RC beams strengthened with externally unidirectional AFRP sheets. Two batches of ready-mixed concrete were investigated. High-strength concrete (HSC) was used for tunnels, and normal-strength concrete (NSC) of the sort usually employed in building construction. The most significant observed increase in the AFRP-strengthened NSC strength was 8.5%, occurring after 360 days of immersion and not exceeding 6.5% in other conditions [64].

Consequently, Zhou et al. [65] found that after high-temperature exposure up to 300 °C, a 55% decrease in peel and shear interface fracture toughness of the AFRP bonded to concrete was recorded. Moreover, the flexural stiffness increased proportionally according to the number of layers of the AFRP sheets compared to the un-strengthened beam [66]. Additionally, prestressed strengthened beams showed higher stiffness than the non-pre-stressed counterparts at the same amount of reinforcement [66].

Basalt fibers (BF), formed from volcanic lava freezing on the earth's surface, are an inexpensive, eco-friendly material with excellent insulation properties and an environmentally friendly alternative to glass and carbon fibers [67]. Incidentally, Sim et al. [68] examined how BF reinforcement boosted the beam samples' ultimate and yield strength by up to 29%, depending on the number of BF layers. Moreover, the BF reached its maximum capacity before failure when utilizing one or two BF layers. Conversely, Stephen et al. [69] created finite element (FE) models to calculate the gradient of deflection of RC beams under flexural load when strengthened by EB-basalt reinforcement. They found that the flexural capacity of basalt-reinforced beams was higher than those reinforced with steel or FRP ones.

The hybrid combination of FRP (HFRP) composites effectively integrated both strength and ductility of several types of fibers. By the way, Hosny et al. [70] studied the behavior of RC beams strengthened with hybrid CFRP and GFRP (HFRP) laminates. The strengthened beams attained a 10.3% rise in their ultimate bearing capacity compared to their CB. Moreover, Attari et al. [71] found that the RC beams strengthened with a double layer of HFRP composite material recorded a 114% increase in strength capacity compared to their CB. As shown in Table 1, Hawileh et al. [53] found that when the RC beams were strengthened with EB- hybrid GFRP and CFRP, their load capacities increased by 30–98% as compared to those of single-layered CFRP/GFRP sheets. Consequently, Choobbor et al. [72] illustrated that using CFRP/BFRP composite sheets for reinforcing RC specimens improves the beam ductility and rise in the beam's ultimate carrying capacity by 28–75%, corresponding to their CB.

Hosen et al. [55] found that the load-bearing capacity enhancement was between 100 and 160% for side external bonded (S-EB) strengthened RC beams with 0.0071 and 0.005 reinforcing ratios, respectively. Subsequently, Salama et al. [47] demonstrated that S-EB strengthening appeared to be slightly less efficient as a strengthening tool than soffit bonding (Table 1). In contrast, using EB-wrapped GFRP composites to strengthen RC beams seemed to be a successful way of boosting the flexural capacity of RC beams [73]. The beams upgraded with two layers of GFRP fabrics in the tension face with half of both sides below the neutral axis achieved improvements in flexural strength, ductility, and cost efficiency. Moreover, Mostofinejad and Shameli [74] stated that the grooved method (GM) through either end-bonded reinforcement on a groove (EBROG) or embedding end-anchored reinforcement in a groove (EBRIG) proved to be an effective way to increase the ultimate load-bearing capacity. The GM increased the maximum load capacity by 139%, 148%, and 99% for one, two, and three EBROG layers, respectively, and by 142%, 186%, and 155% for one, two, or three EBRIG layers, respectively, compared to U-wrapping EB technique without any surface preparation. Conversely, Nader et al. [56] studied the behavior of RC beams strengthened in flexure using prestressed-CFRP plates via the EBROG method. The use of EBROG prestressed CFRP plates revealed beneficial effects on their stiffness due to the initial prestress applied in addition to displacement delay during the cracking stages of the beams. Moradi et al. [75] proposed a new technique involving perforating holes along the beam webs and inserting FRP reinforcements filled with grout. The beams were strengthened by EB-FRP reinforcement and embedded-through-section FRP reinforcement. The maximum load and displacement of the strengthened beams with embedded FRP strips in holes drilled through the beam web were higher by 70.9% and 15.6%, respectively, than those reinforced with EB-FRP reinforcement U-wrapping strips.

RC beams strengthened with EB-natural FRP (NFRP)

Climate change has made natural fiber-reinforced polymers (NFRPs) an appealing alternative to synthetic FRPs [76]. NFRP-flax is a popular choice among these raw materials due to its low cost, lightweight, relatively high strength, and stiffness for structural applications. The NFRP laminates and concrete possess similar elasticity. The NFRP-strengthened RC beams failed by FRP rupture and recorded higher ultimate loads and ductility than the CFRP-strengthened beam [77]. Moreover, coir fibers had the most significant strain at fracture [77]. Samples comprised of two types of NFRP (flax and jute) were tested by Chen et al. [48]. They found that the beam load-carrying capacity with flax-FRP (FFRP) increased by 40% compared to CB, and it also showed higher

load-carrying capacity than those used jute-FRP (JFRP), as shown in Table 1. Moreover, the beams strengthened with eight layers of fabrics recorded the highest load-carrying capacity (103.7 kN). Huang et al. [49] investigated the flexural performance of RC beams with EB-FFRP plates. The experimental variables included FFRP thickness (4 and 6 layers), steel reinforcement ratio (0.223% and 0.503%), and the pre-cracking of RC beams before bonding the external FFRP plates. They demonstrated that EB-FFRP laminates increased the load-carrying capacity by 15–112%, while the ultimate mid-span deflection ranged between 92.3 and 147.4% from those of the CBs. As shown in Table 1, the maximum load and ductility increase was more pronounced for RC beams with a lower steel ratio. Conversely, Wang and Chouw [78] tested coconut-FRP (CFRC) specimens strengthened with various thicknesses of FFRP (2, 4-and 6-layer). The coconut fiber content in the mixture was 3% of the cement mass, corresponding to an approximate fiber volume content of 1.2%. The results showed considerable enhancement in the flexural strength and impact resistance for beams reinforced with EB-FFRP. They found that the flexural strengths of the FFRP-CFRC beams with 2, 4, and 6-layers were, respectively, almost 1.7, 3 and 4 times that of CFRC.

On the other hand, natural sisal FRPs (SFRP) are advantageous components for reinforcement due to their low density, high toughness, bio-friendliness, ease of the skin, and biodegradability [79]. Yinh et al. [80] investigated the effectiveness of EB-SFRP on the strength and ductility of concrete. They revealed an increase in the case of polyester resin by 14%, 29%, and 36% for two layers of SFRP, two layers of SFRP with anchorage system, and 4-layers of SFRP with anchorage system specimens, respectively. In the case of epoxy resin, 19%, 45%, and 68% increases in the ultimate load were observed for 2-layers of SFRP, 2-layers of SFRP with anchorage system, and 4-layers of SFRP with anchorage system specimens, respectively. Lastly, Hussain et al. [81] proved that external confinement by using fiber rope-reinforced polymer (FRRP) was very effective in enhancing the concrete's ultimate strength, strain, and deformability. Further, the hemp FRRP composites were more effective in increasing the maximum compressive strength than cotton and polyester FRP composites. Polyester FRRP composites were better than hemp and cotton FRRP from the viewpoint of ultimate strain.

RC beams strengthened with EB-fabric-reinforced cementitious matrix (FRCM)

The fabric-reinforced cementitious matrix (FRCM) systems, commonly called TRM, have recently been utilized in construction as an effective alternative for strengthening materials. FRCM is produced from fabric grids and a cementitious agent acting as a matrix and binder. The cementitious matrix in FRCM has a high thermal capacity [26]. Additionally, the cementitious matrix in FRCM is more compatible with concrete substrates than the epoxy resin with FRP. The mortar matrix used in this system was more adept at resisting heat/fire, creating better bonding between ultra-high performance fiber-reinforced concrete (UHPFRC) and concrete than concrete-to-concrete interfaces [82]. Unlike conventional FRP, FRCM contains continuous high-strength fibers surrounded by a matrix. Paschalis et al. [83] performed an experimental and numerical analysis of UHPFRC strips utilized for the flexural strengthening of entire RC beams. Two beams were strengthened with UHPFRC layers, and two beams were strengthened with UHPFRC layers and steel bars. It was revealed that an increase in load-carrying capacity by about 89% can be achieved by continuously applying steel bars on the layers. Deng et al. [84] investigated the flexural performance of RC beams strengthened by highly ductile fiber-reinforced concrete (HDC) and reactive powder concrete (RPC). They found that RPC-reinforced specimens in the compressive zone had more bearing capacity due to their high compressive and adhesive strengths. In the tension zone, the ultimate flexural strength of specimens strengthened by an HDC layer increased up to 170%, and the cracks were delayed and effectively dispersed. Giese et al. [85] studied how locally manufactured fiberglass textiles (TEX-IGLASS AR 360-RA 04) affect the flexural strengthening of RC beams. They observed growth in the ultimate load of 31%, 54%, and 72% for 2, 3, and 4 layers, respectively. Conversely, Alharthi et al. [86] studied a new technique to strengthen RC beams using a limited steel-bar-reinforced mortar layer (SBRML). They observed an increase in the ultimate load by about 113% compared to the CB when using SBRML. This method was suitable for RC elements with small widths and without concrete cover (CC).

RC beams strengthened with EB-Steel meshes.

Compared to FRP, hardwire steel-fiber (HSF) as external reinforcement has more advantages [52]. These include increasing stiffness, bond, and strength performance due to its high modulus of elasticity and tensile strength. Additionally, HSF composite sheets are lighter and more economical than conventional FRP laminates. Furthermore, they can be pre-stressed easily. Conversely, Xing et al. [87] found that using steel wire meshes (SWM) and polymer mortar composites to strengthen RC beams can efficiently increase their flexural capacity. All reinforced beams were stiffer than the CB and could bear a greater load capacity. Alternatively, Hawileh et al. [52] explored EB-strengthened RC beams with medium and high-density embedded HSF sheets via epoxy adhesives. They found a 62% load-bearing capacity improvement over the CB with two layers. Otherwise,

Qeshta et al. [88] demonstrated that the RC beams loaded in flexure and strengthened with SWM and CFRP sheets and a hybrid combination of the two materials eventually failed due to rupture of wire mesh or debonding of laminates. The test results revealed an increase in the first crack and yield strength by 90% and 47%, respectively, compared to specimens strengthened with SWM. High or low cord-density galvanized steel mesh (GSM) sheets can be EB to RC structures using epoxy adhesives. However, only meshes with low cord-density GSM sheeting are suitable for combination with cement mortar [89]. In contrast, Douier et al. [89] observed that the ultimate-flexural load capability increased by 41.8–51.4% when reinforcing the RC beams with GSM sheets. In contrast, no increase in strength was detected when comparing anchored specimens without prior strengthening against strengthened specimens that were anchored beforehand.

RC beams strengthened with EB-metal plates

Rasheed et al. [51] examined how Aluminum Alloy (AA) plates could act as EB flexural reinforcing for highly RC parts. The results were compared with a CB without CFRP sheets which doubled up as an anchorage U-wrap system. As shown in Table 1, the increase in strength showed a variance from 13 to 40%. Subsequently, Abdalla et al. [50] ascertained that utilizing AA plates can significantly increase beam shear capacity. This occurred when they were oriented at 45°. An increase in strengthened RC beam ductility and load-carrying capacity by about 39% compared to the CB was recorded, as shown in Table 1. Moreover, Abuodeha et al. [90] studied the flexural behavior of RC beams strengthened using AA plates with two anchorage techniques: bonding only and bolting plus bonding. They found that the beams strengthened with bonded AA plates demonstrated a 32% increase in load capacity. In contrast, those featuring bolted AA plates incited only a 24% improvement over the CB.

RC beams strengthened with EB-hybrid-bonded FRP technique (HFB-FRP)

A practical solution to the debonding problem is the utilization of HFB-FRP, which uses a steel plate as a mechanical fastener fixed with rods and nuts associated with it rather than pins [91]. Also, Zhou et al. [92] observed that utilizing this system prevented debonding issues within FRPs and increased the ultimate load-carrying capacity of beams up to 2.13 times compared with the U-jacketing strengthening technique. Moreover, Zhang et al. [93] point out that FRP debonding failure is a preferred mode in the HFB-FRP combination due to its good ductility, solving the issues faced by EB-FRP strengthening. Hence, the mechanical fastening technique (MF) was

suggested to be an efficient alternative to EB techniques, providing cheap and speedy, reliable flexural reinforcement [94]. Consequently, Ebead [95] showed that specimens strengthened with a hybrid EB/MF-FRP system exhibited more significant increases in P_y and P_u than those using the MF-FRP system, ultimately achieving 60% to 125% of the load-carrying capacity of the un-strengthened specimen. Moreover, Hadhood et al. [96] noticed the failure envelope of the RC beams strengthened with a hybrid technique consisting of EB/MF and reduced-size CFRP strips. The beam brought about a 65% improvement in the shear load compared to the CB. Finally, Zhou et al. [54] proposed a mixed anchoring technique that blended EB and ended anchorage for FRP sheets. These have been self-locked into slotted plates, which are then attached to concrete via pre-planted bolts. This technique improved the ultimate strength, enhanced the failure ductility, and resulted in either FRP rupture or concrete crush despite a debonding degree, as shown in Table 1.

Modes of failure of RC beams strengthened with EB reinforcement

Figure 2 and Table 1 show the failure modes denoted by a series of letters representing steel yielding (S), concrete crushing (C), FRP rupture (Fr), and FRP deboning (F). For example, SC means that steel yielding is followed by concrete crushing, while SF indicates that steel yielding happens before FRP debonding. Lastly, in the case of SCF, steel yielding happens before concrete crushing, and FRP clambering failure occurs afterward. Most research on RC beams strengthened with FRP reported failure due to delamination or debonding of the FRP [47, 52, 53, 80, 97]. The same issue was pointed out in ACI 440.2R-08 [98], which reported that cover delamination or FRP debonding could occur if the substrate cannot sustain the force exerted by the FRP.

Steel yielding followed by concrete crushing (S-C)

In the S-C failure mode (Fig. 2a) commonly seen in CB, the cracking initiated at the concrete tension zone and then propagated vertically toward the compression zone resulting in compression failure [53, 55, 60]. Consequently, steel yielding was discovered as diagonal cracks advanced toward the loading points on the shear span [49, 56]. Afterward, no more cracks were observed; eventually, the concrete in the tensile zone began to peel off, leading to the failure of the beam [47, 52, 80]

Steel yielding followed by concrete crushing and FRP debonding (SC-F)

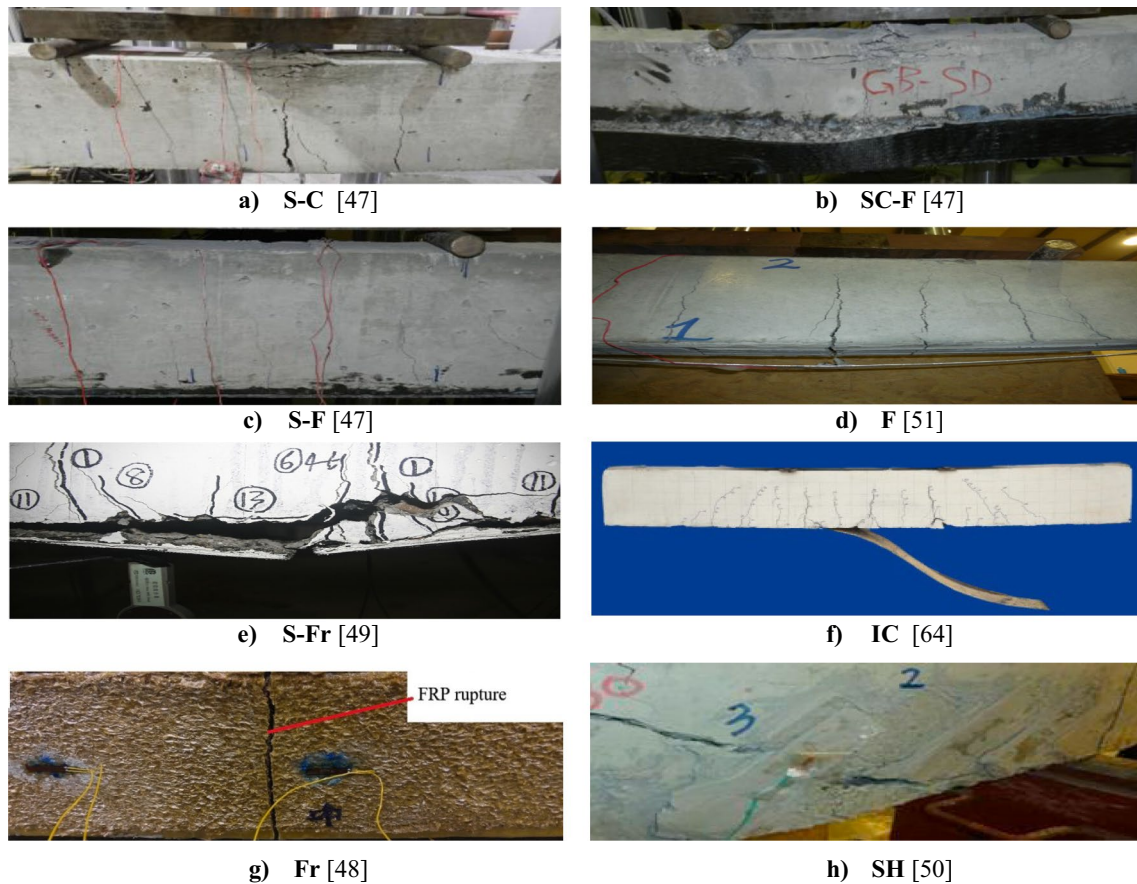In the SC-F failure (Fig. 2b), the micro-cracks near the interface of the beam are the first signs of debonding.

Fig. 2 Failure modes in the EB strengthening method

With further loading, a major diagonal crack is formed and spreads along the interfacial concrete quickly, causing the delamination of FRP layers. The bond cracks in the middle of the beams propagate at an angle of around 45° and then reach out to either side, causing concrete cover separation [56, 99]. Consequently, Salama et al. [47] observed the occurrence of steel yielding before CFRP debonding with minor concrete crushing for single-ply strengthened beams. Hosen et al. [55] stated that the delamination of the CFRP fabric initiated the failure, followed by a gradual decrease in the applied load until failure occurred due to concrete crushing in the compression zone. Moreover, Hawileh et al. [52] found that due to high-stress concentrations around the HSF ends, horizontal shear cracks are formed, followed by the splitting of the concrete cover. Also, Hawileh et al. [53] observed the occurrence of concrete crushing beneath the loading supports.

Steel yielding followed by FRP debonding (S-F)

The S-F failure mode (Fig. 2c) involves FRP debonding (Fig. 2d) for specimens strengthened with soffit and side-bonded FRP [47]. The failure resulted in shear cracks with no concrete crushing due to debonding of FRP laminates, followed by a sudden dropping in load-carrying capacity [97]. On the other hand, Hosen et al. [55] noticed shear cracks intersecting flexural cracks, which caused delamination of S-EBR CFRP fabric. According to Hawileh et al. [53], the formation of vertical shear cracks from both sides of the beam caused CFRP sheet debonding. Also, Yinh et al. [80] observed this type of failure when studying sisal-FRP strengthened RC beams without end-anchorage.

Steel yielding followed by the rupture of the FRP plate (S-Fr)

For S-Fr failure (Fig. 2e), initial, short, and thin cracks appear through the beam vertical section at the mid-span. Then, the cracks increase in number and size and become symmetrical. Afterward, more defects, such as steel yielding, are formed with horizontal cracks in the concrete tension zone due to the FRP plates and concrete gap. Additionally, thin cracks are observed on the compression side of the concrete. After a further increase in the applied load, a slight noise was heard from the FRP plates, and diagonal cracks became noticeable more quickly. As

an extra increment in load is applied to this shear span, louder noises can be heard from the FRP strips. In conclusion, these tensions eventually caused the beam to fail due to FRP rupture within the beam mid-span [61]. However, large amounts of concrete substrates are attached to the FRP plate, and both ends of the FRP bands did not cause damage due to reinforcement supplied by FRP [49].

FRP deboning by an intermediate crack (IC)

The FRP reinforcement in the beam failed to delaminate due to IC debonding (Fig. 2f) that initiated near the loading zone and spread to the edge of the FRP material at supports. The concrete in the compression section did not crush. In this type of failure, the CFRP sheet acts as a bridge over the crack and prevents it from further extending [47, 55, 100]. El-Sayed et al. [60] noticed a peeling action that led to failure to strengthen shallow RC beams with bottom CFRP layers. Similarly, Yin and Wu [61] showed that, when analyzing steel-fiber RC specimens strengthened by CFRP with 0.25% and 0.5% steel-fiber volume fractions, the IC debonding failure gradually results in large deformation as the deboned region goes toward curtailment of the FRP. More considerable mid-span deflections occur upon final failure for experiments with many NFRP layers [48]. IC debonding failure mode was also observed in AFRP-strengthened beams [64]. Before reaching the final failure of sisal-FRP strengthened beams with end anchorage systems, no pullout of anchors or debonding of sisal-FRPs occurred, but the beams collapsed due to the inclined cracks created around the loading and anchoring points [80].

FRP rupture (Fr)

In Fr mode (Fig. 2g), the beam fails due to the sheet rupture [20]. The ultimate deflection at the midpoint of the beam was less than that of the reference beam. This is because the strain at fracture of the FRP is less than its maximum strain capability (the ultimate strain of the FRP strip) [47]. Previous studies [61, 66] highlighted that even though peeling-off areas were visible, the FRP sheets adhered very well to the surface of concrete beams strengthened by CFRP with a steel-fiber volume fraction of 1% or by AFRP sheets.

Shear failure -brittle failure (SH)

Tests conducted on beams under four-point bending resulted in a shear failure (Fig. 2h), where inclined cracks begin at the loading points and proceed toward the nearest support [50, 75, 101]. Ebead [95] demonstrated that these diagonal cracks arise due to progressive ductile flexural behavior related to fastening. Hadhood et al. [96] showed that using the MF technique and EB could hinder the emergence of any shear cracks. Therefore, cracking formed under the strips near the left support before widening.

Strain response

Table 2 illustrates the ultimate FRP Strain ($\mathcal{E}_{fu}$), the maximum FRP strain for the EB-strengthened beam under flexural ($\mathcal{E}_m$), and the efficiency of the strengthening elements. After the steel rebar yielded, two factors enhanced the load resistance (increasing the strain in the FRP laminates and the strain hardening of the steel rebar), although the latter had a low effect. Chen et al. [48] reported that, after yielding, most load resistance comes from the FRP laminates due to their high tensile strain. Moreover, El-Sayed

Table 2 The maximum FRP strain for EB-strengthened beam under flexural

Author	Specimen	$\mathcal{E}_m$ (με)	$\mathcal{E}_{fu}$ (με)	Strain efficiency%
El-Sayed et al. [60]	Pultruded CFRP plates (Thickness and width are 1.4 mm and 120 mm)	6367	16,970	37
Salama et al. [47]	Single Ply Bottom V-wrap C200H unidirectional CFRP sheets,	8000	21,230	37
Zhang and Wu [64]	AFRP sheet made of the fabric and exposed to salt water for 360 days	14,775	16,839	87
Ferrier et al. [103]	Composite fiber cement internally reinforced by CFRP rods (CFCIR–CFRP) with- Pre-stressing	10,841	17,692	61
Tehrani et al. [56]	EBROG Plate M514 Quantum CFRP plate with 50×1.4mm with 30% of prestressing strain	13,011	15,000	86
Razaqpura et al. [104]	Sika CarboDur S512 CFRP laminate with 30 $\pi-$ anchors	13,675	16,970	80.4
Attari et al. [71]	1 Layer GFRP SikaWrap430G + 1 Layer CFRP SikaWrap230C U Shape	14,100	14,285	98
Xiong et al. [105]	1-layer of CFRP sheet (50 mm wide and 0.11 thickness)+1-layer GFRP sheet (62.5 mm wide and 0.167 mm thickness)	17,800	19,197	73
Qeshta et al. [88]	hybrid of wire mesh-epoxy and CFRP sheet	19,528	21,000	93

et al. [60] found that at failure, the CFRP plates achieved a strain of 6367 μ$_ε$ which represented 37% of its ultimate strain. Conversely, Ebead [95] observed lower strains in FRP strips than those in steel reinforcement for beams strengthened with EB/MF. Moreover, the slip was caused by either fastener rotation or bearing damage in the strips. Alternatively, Salama et al. [47] reported that steel bars yielded before failure in all specimens, and none reached the ultimate rupture strain of the CFRP. There were 8000 and 7400 μ$ε$ levels for single-ply samples at 190 and 195 kN maximum loads, respectively. The strain levels in Double-ply were lower by 3400 and 6100 μ$_ε$ at 225 kN and 217 kN ultimate load, respectively. Also, Abdallah et al. [5] found that replacing EB-CFRP sheets with CFRP plates significantly reduced the maximum tensile strain of the CFRP and lowered the possibility of extending its capability.

Ali et al. [62] highlighted the more significant properties affected by strengthening using CFRP sheets. It was found that as the vertical deflection of the beam increased, the strain spread from its center to the supports due to IC-induced debonding. Furthermore, a continuous RC beam reinforced with CFRP exhibits an increased elastic limit capacity compared to a beam strengthened with GFRP sheets [102]. Moreover, Huang et al. [49] suggested that the increase in FRP layers leads to a higher ultimate strain and six layers recording maximum strain up to 1.93%. There was a remarkable increase in stiffness for beams strengthened with HSF sheets. Furthermore, Hawileh et al. [52] found that lamination of HSF having a width of 120 mm failed at 0.0032 strain which was lower than other specimens due to its higher stiffness and larger contact area of the HSF sheet with the specimen's soffit. Alternatively, Nader et al. [56] revealed that using CFRP anchorage increased the strain of prestressed beams by 20%. The anchorage allows higher shear forces to be achieved, thus leading to slightly higher strains in the stirrups and better performance of the CFRP sheets [101]. The maximum stirrups strain measured for specimen strengthening by S-EB strips of woven carbon fiber fabric and U-wrapping externally bonding was lower than the failure strain of FRP. This may indicate that these methods cannot ensure that the total strain capacity of the FRP will be utilized. So the beam will not reach its expected maximum shear capacity [75]. Otherwise, Hawileh et al. [53] showed that GFRP/CFRP/GFRP hybrids had a lower failure strain than the GFRP/CFRP specimen due to concrete crushing under flexural forces in constant moment zones. From the previous, the GFRP showed the highest strain efficiency [71], followed by a hybrid of wire mesh-epoxy [88] and AFRP [64], while the CFRP [47, 56, 60, 103, 104] showed the lowest strain efficiency (Table 2). This ensured that the lower the young's modulus of the strengthening elements, the higher the strain efficiency.

Ductility analysis

Deformation is another crucial aspect of flexural behavior. The beam's ductility can be quantified by measuring the mid-span deflection relative to the steel yield point. This measurement was established by examining the corresponding flexural strain gauge readings and load–deflection curve, as well as indicating the level of plasticity that a beam can resist before failure. The beam's ductility indices are computed at the ultimate attained load ($\mu_{\Delta u}$) and failure load ($\mu_{\Delta f}$) as follows:

$$\mu\Delta u = \frac{\delta_{ult}}{\delta_y} \tag{1}$$

$$\mu\Delta f = \frac{\delta_f}{\delta_y} \tag{2}$$

Table 1 shows that the CB demonstrated the highest ductility among all tested beams. The ductility index decreased as the reinforcement ratio for EB-strengthened RC specimens increased. With increased CFRP layers, a drop in the ductility of strengthened beams was observed [47–49]. This outcome has been demonstrated by Hawileh et al. [53], who found that hybrid sheets led to 17.8% higher strength and ductility than a beam strengthened with a single carbon sheet. Additionally, Xiong et al. [105] observed that the ductility of hybrid CF/GF beams was 89.7% higher than others under similar failure loads, with 10% lower stiffness and 38% lower cost than CFRP-strengthened beams. This reduced the cost by 16.2% as compared to the CB. According to Choobbor et al. [72], the ductility indices of the RC beams strengthened in flexure by hybrid BFRP/CFRP sheets presented a maximal improvement of up to 108% compared to specimens reinforced with CFRP laminates alone. For the beams strengthened with the same number of layers, an increase in basalt sheets of the hybrid laminate achieved higher ductility up to 31.1% [72]. Deng and Xiao [66] demonstrated that an un-prestressed AFRP sheet produced nearly the same ductility performance as the CB. However, prestressed AFRP sheets reduced their ductility; therefore, they should be employed carefully in seismic zones. Both Chen et al. [48] and Huang et al. [49] revealed that FFRP reinforcement highly affected the ductility of RC beams, and more FFRP layers showed better deformability and ductility until the final failure. Hosny et al. [70] found that combining CFRP and GFRP resulted in higher ductility than beams strengthening with one FRP lamination by about 2.4%. Giese et al. [85] found that the decrease in ductility ratio for the two and three layers varied between 2.45 and 2.84, while four layers reached a ratio of 3.25.

Hileh et al. [52] showed that the ductility of HSF-EB strengthened beams (medium and high-density) at the ultimate load ($\mu_{\Delta u}$) and failure load ($\mu_{\Delta f}$) was less than that of the CB by 54–70%. However, unlike RC beams reinforced with FRP, those strengthened with AA plates demonstrated similar yield-ductile behavior as the CB. In the long run, this behavior is expected to be enhanced compared to steel due to the anti-corrosive effects of AA plates. Also, the end anchorage provided equivalent ductility levels to that observed for the CB as it increases deformation beyond the nominal debonding strain values [51]. The ductility index for beams strengthened with AA-EB plates decreased compared to the CB [50]. Beam with EB-AA plates showed a 45% increase in deflection compared to the CB, whereas using bolted and bonded AA plates recorded an 84% increase in deflection compared to the CB [90].

The ductility index of the S-EBR lightweight strengthened specimens decreased by 49% [55]. According to Salama et al. [47], the decrease in ductility at ultimate and failure loads in the soffit and side-bonded strengthening systems ranged from 42.3 to 55.6% and 45.5 to 62.5%, respectively. Furthermore, adding CFRP anchors and securely bolting them to the strengthened RC beams could help to increase their ductile properties, thus delaying or avoiding the debonding of the sheets altogether. Ebead [95] found that specimens strengthened with EB/MF-FRP had more brittle behavior than samples strengthened with MF-FRP. Installing end U-Wrapped anchored on GSM bonded with mortar, the ductility increased to 142.1% and 270%, respectively, compared to the control and non-anchored specimens [89]. However, compared to CB and non-anchored samples, intermediate anchored specimens had 134.1% and 257.3% increase in ductility, respectively. Furthermore, using the EBROG method instead of EBR strengthening caused an enhancement in ductility by 53% due to delayed CFRP debonding [56]. Escrig et al. [106] found that using FRCMas and EB-strengthening decreased the ductility of RC beams. They also showed that beams strengthened using steel experienced the most significant decrease in ductility compared to basalt, carbon, and glass [106].

Parameters affecting the flexural behavior of EB strengthened beams

The type and the amount of FRP

El-Sayed et al. [60] showed that increasing steel-fiber volume fraction and using multiple FRP layers in the EB technique increases stress transfer lengths and ultimate loads. Salama et al. [47] confirmed that the beams strengthened with 2-plies of side-bonded CFRP laminates had up to 93.4% more flexural strength than CB. As the number of CFRP layers increased, the ultimate strength of reinforced

high-strength concrete continuous beams strengthened with both CFRP and GFRP sheets enhanced, as shown in Table 1. However, this is accompanied by decreased ductility, moment redistribution capabilities, and ultimate strain for the CFRP sheet [62]. Abdallah et al. [5] suggested that increasing the CFRP weight per unit area could be an effective alternative to multiple layers reinforcement. This depends on the beam's total axial stiffness ratio and the adhesive resin.

Conversely, the FFRP plates could achieve a similar impact on the beam's ultimate lateral load-carrying capacity as GFRP, CFRP, and steel plates [48, 49]. Deng and Xiao [66] found that when the number of the prestressed AFRP layers increased, there was an associated increase in bearing capacity. However, this increase was inconsistent with the number of AFRP sheet layers. Four layers of NFRP laminates (with 6.67 times the sectional area of CFRP laminates) proved to have the best advantages concerning strength, cost-effectiveness, and environmental considerations [107]. At the same time, larger cracking loads were observed when the thickness of NFRP was increased [80]. This is owing to the higher stiffness of thick sisal-FRP (4 layers) compared to thin sisal-FRP (2 layers), which resulted in a loading increase of 73% and 100%, respectively, compared to CB.

The effective bonded length

Chen et al. [48] found that jute-FRP was shorter than CFRP and flax-FRP, making jute-FRP more susceptible to FRP rupture. RC beams with CFRP plates covering at least 25% of their shear span paired with the correct type of end anchorage was demonstrated as an effective strengthening leading to reduced costs and materials [58].

The width of FRP sheets

The centroid of the sheets setting closer to the section's neutral axis reduces the CFRP's sheer depth and moment arm, which reduces the efficiency of the S-EB reinforcing the RC beams [48, 52]. Salama et al. [47] reported that the ultimate loading levels of beams strengthened with 50 mm, 100 mm, and 150 mm wide CFRP sheets increased by 39.7%, 66%, and 87.2%, respectively, compared to the CB.

Strengthening direction

Reinforcing non-pre-cracked and pre-cracked palm oil clinker lightweight RC beams with S-EB CFRP laminates improved their load and flexural capacity [55]. Moreover, Panigrahi et al. [108] and Alternatively, Abdalla et al. [50] emphasized that the strips tilted at 45° provided greater efficiency than vertical strips. In contrast, Salama et al. [47] noted that side-engagement of CFRP fabric is less effective

than conventional soffit strengthening concerning flexural properties and the strength of RC beams. As centroid depth can affect the moment arm of force in a beam's cross-section, it was observed that once the fabric separated on one side, the load would be shifted over, leading to a brittle failure mode [47].

The environmental effects

Figure 3 illustrates how immersion in 35g/L NaCl solution for a year had not significantly affected the load capacities for beams strengthened with AFRP. Furthermore, specimens immersed for 360 days registered the highest average rise (up to 8.5%) [64]. According to Wroblewski et al. [99], further enhancement in the beam load was obtained using dry heat due to the increase in the cross-linking density of the bonding polymer.

Externally bonded reinforcement on grooves (EBROG)

The specimens strengthened by the EBROG method displayed a higher load-bearing capacity, ductility, and CFRP debonding strain when compared to those treated with EBR [56, 74, 109]. Additionally, the experiments showed that the performance of EBR in the groove (EBRIG) strengthening was stronger than the EBROG strengthening when only one layer of longitudinal CFRP was used. In contrast, EBROG was more efficient than EBRIG when multiple layers of CFRP sheets were employed [74].

Anchorage systems

The role of anchorages in the failure process is essential as the beams have no anchorage yielded to debonding of the plate ends. In contrast, the EB with end anchorage produced localized debonding between the anchors. Wang and Hsu [110] showed that the U-wrap with end anchorage was the

Fig. 3 Flexure strength for AFRP-strengthened NSC and HSC beams after different immersion times [64]

most successful configuration. Moreover, Yinh et al. [80] found an increase in the ultimate loads of strengthened RC beams by 13% and 21%, respectively, when polyester and epoxy resin was utilized to install the sisal-FRP strengthening with end anchors. Additionally, Abuodeha et al.[90] found that bolting could significantly increase the beam ductility. However, using a bolted and bonded AA plate had a lower load capacity than the bonded AA plate due to drilled holes. The holes resulted in a reduction in the cross-section area and thus lowered its contribution under load.

Consequently, Hadhood et al. [96] revealed that increasing the number of fasteners would intersect cracks and improve the bond between the CFRP strips and concrete surfaces. Also, the EB/MF technique achieved similar strength and stiffness as the specimen with full-length EB strips and reduced the strengthening area of CFRP by 44%. Moreover, Oller et al. [101] stated that anchoring FRP sheets was necessary to achieve an effective result since premature debonding occurred if no anchors were present. Consequently, Rasheed et al. [51] reported that when end anchorages were used with EB-AA plates to reinforce the RC beams, the strength was not improved while the beams' ductility increased. In addition, Razaqpur et al. [104] expressed that strengthening the RC beams with 1.2 mm thick and 50 mm wide CFRP laminate and adding π-CFRP anchors improved load-bearing performance by more than 20.8% compared to those without anchors. Also, Zhou et al. [54] proved that self-locking anchorages could improve the ultimate capacity and failure ductility of the RC beams strengthened by EB FRP, thus avoiding end debonding and restraining intermediate crack debonding development.

Epoxy

The importance of selecting the proper epoxy for FRP strengthening was demonstrated, particularly in a marine environment. Using polyoxy-propylenediamine hardener/epoxy resin to bond an FRP sheet to the tension side of a concrete beam resulted in higher flexural strength and ductility than a modified amine/epoxy resin blend or an amine saturant/solvent-free epoxy at room temperature [111]. However, too much epoxy resin negated the environmental benefits of natural fibers [107]. Consequently, Yinh et al. [80] found that sisal-FRP with epoxy resin had better mechanical properties than sisal-FRP with polyester resin, increasing the ultimate load by 36% compared to the CB. On the other hand, the maximum load for beams strengthened with NFRP using epoxy was 68% more than the control beam.

Cost-efficiency

The high proportion of epoxy resin in the composites made the cost advantage of natural fibers relative to carbon fiber
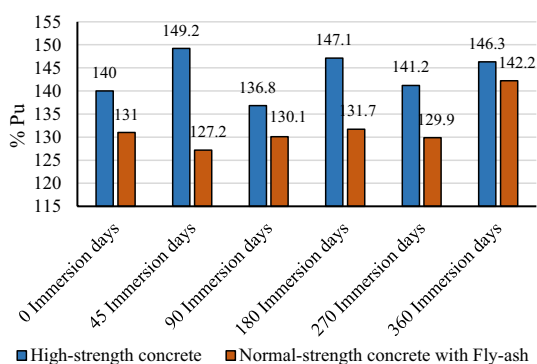
negligible [107]. The most significant beneficial effects and cost-effectiveness were noticed when using unidirectional flax, among other synthetic and natural fibers [48].

Flexural behavior of the strengthened beam with NSM reinforcement

Summary of existing studies related to the NSM technique

Table 3 shows some existing research treated with the members strengthened with NSM strengthening. Al-Issawi et al. [112] observed that reinforcement of beams with an a/d ratio of 0.85 improved load capacity from 7.35 to 20.56% (a = the shear span length and d = the beam depth). For beams with an a/d = 1.136, the increase in the load ranged between 8.13 and 15.45% (Fig. 4). Moreover, Khalifa [113] compared the NSM and EBR techniques as flexural strengthening for RC beam (Fig. 5) and reported that when the same amount of CFRP was utilized, the ultimate load of beams reinforced with NSM was 12–18% higher than those with EBRs. Alternatively, Ebead and El-Sherif [114] investigated the effect of three different FRCMs with fabric plies material (polypara-phenylene benzobisoxazole (PBO)/carbon/glass) as NSM and EB strengthening technique. The findings indicated that the FRCM-NSM and FRCM-EB increased the load of strengthened beams by 62.5% and 72.3%, respectively.

Hong and Park [116] investigated the effect of various prestress levels on the flexural behavior of concrete beams strengthened with prestressed NSM CFRP reinforcements. They found that as prestress levels increased, the cracking, yield, and ultimate loads of the RC beams strengthened with NSM-FRPs increased (Fig. 6). A minor prestressing effect on the deflection was noticed at cracking and yield load. However, the ultimate deflection was significantly affected by prestressing. It was recommended that the concrete beams should be subjected to a prestress level of 50% only from CFRP rupture strength. Likewise, El-Gamal et al. [119] investigated the flexural behavior of RC beams strengthened with NS-FRPs (CFRP or GFRP) using two techniques (NSM or hybrid). Also, the effect of the FRP amount (one or two bars) and the tension steel reinforcement ratio were investigated. They found that doubling the FRP amount amplified the ultimate capacity by about 85% (Fig. 7). Also, NSM-GFRP upgraded beams showed a respectable ductile response. Alternatively, Kotynia [126] concluded that the internal steel reinforcement influenced the FRP-concrete bond performance. In RC elements, the concrete failure plane shifts from having a trapezoidal shape (in clear concrete) to almost horizontal, either along or slightly beneath the longitudinal steel support. Conversely, Almusallam et al. [120] found that using NSM steel or GFRP bars with

sufficient end anchorage could effectively restore the load capacity of RC beams with corroded steel reinforcement.

Moreover, Sharaky et al. [117] reported that yielding loads in CFRP and GFRP beams increased by 50% and 29%, respectively, while the ultimate loads increased by 66% for CFRP and 60% for GFRP. Moreover, the NSM technique effectively increased RC beams' load capacity and stiffness depending on the NSM material. Conversely, by increasing the number of NSM-CFRP bars from one to two bars, the yielding and the maximum loads increased by 25.6% and 7.5%, respectively. Also, doubling the NSM-GFRP bars increased the yielding and maximum loads of the beams by 11.7% and 13%, respectively, over those strengthening with one GFRP bar (Fig. 8). Alternatively, Al-Mahmoud et al. [6] concluded that CFRP rods were remarkably successful in increasing the flexural strength of RC beams, regardless of whether resin or mortar was used as a filling material. The beam strengthened by CFRP rods with mortar displayed a debonding from the groove. Conversely, Sakar et al. [127] also demonstrated that GFRP rods create an effective NSM strengthening system, enhancing RC members' load capacity and ductility under cyclic loading.

Qin et al. [128] studied the influence of environment and fatigue load coupling and uncoupling on the RC beams strengthened with CFRP. Their outcomes revealed that a hot-wet climate significantly affects the fatigue and durability behavior of RC structures strengthened with CFRP. When humidity was stable, the relative fatigue limit decreased as temperature consistently heightened. Likewise, when the environment temperature stayed constant, the relative exhaustion threshold diminished as the moisture content elevated. Moreover, MRasheed et al. [129] investigated four different strengthening methods: EB CFRP sheets, EB-steel-reinforced polymers (SRP) sheets, and NSM CFRP and NSM stainless steel bars. They declared that external FRP transverse strengthening could accomplish ductile flexural response to avert the flexure system's premature debonding and delamination failure. Furthermore, Lee et al. [130] looked into the impact of the prestressed NSM-CFRP system on the strengthened RC beams. They investigated the influence of prestressing method, type of filler, surface treatment of the CFRP bar, and number of bars on the flexural behavior of RC beams. It was found that having greater prestressing forces applied to the RC beam improved the strength and increased the ultimate load at which cracking occurs. They also hinted that post-tensioned NSM strengthening systems could be used to strengthen cracking resistance. The pretensioned NSM-strengthened RC beams with 2 bars showed an increase in concrete cracking, steel yielding, and maximum loads by about 17.8%, 8.4%, and 2.8%, respectively, compared to one bar. Similarly, Kara et al. [131] concluded that strengthening RC beams with prestressed NSM FRP improved their cracking and yielding loads by increasing

Table 3 Studies on RC beams strengthened with NSM strengthening

Authors	Method and filling	Specimen designation		% P_u	Δy (mm)	Δu (mm)	Failure Mode	$\mu_{\Delta u} = \delta u/\delta y$
Al-Issawi et al. [112]	NSM CFRP bars according to the (a/d) ratio	a/d=0.85, Ø8 mm CFRP, vertical inclination	150 mm spacing	7.35				
			100 mm spacing	10.29				
		a/d=0.85, Ø12 mm CFRP	150 mm spacing vertical inclination	14.70			SH	
		a/d=0.85, Ø8 mm CFRP, inclined by 45°	150 mm spacing	13.97			S-Cs	
			100 mm spacing	20.59			S-Cs	
		a/d=1.136, Ø8 mm CFRP, vertical inclination	CB	–			SH	
			150 mm spacing	8.13			S-Es	
			100 mm spacing	12.2			SCS	
		a/d=1.136, Ø8 mm CFRP, 150 mm spacing	inclined by 45°	14.63			F	
			inclined by 30°	15.45			S-Cs	
		a/d=1.42, inclined by 45°, 150 mm spacing	CB	–			SH	
			Ø8 mm CFRP,	8.7			S-Cs	
Zhang et al. [115]	NSM BFRP and NSM GFRP bars with various bonded lengths (BL)	Ø8 mm BFRP, C30 MPa	BL=100	4		12.72	S-Es	
			BL=200 mm	–		10.35	F-C	
			BL=300 mm	12		13.85	F-C	
			BL=400 mm	14.5		17.01	F-C	
		Ø8 mm GFRP, C30 MPa	BL=100 mm	7		16.03	S-Es	
			BL=200 mm	3		14.37	F-C	
			BL=300 mm	9		17.58	F-C	
			BL=400 mm	8		18.52	F-C	
		Ø10 mm GFRP, C30 MPa	BL=100 mm	7.7		6.05	S-Es	
			BL=200 mm	6.11		7.92	F-C	
			BL=300 mm	17.65		9.96	F-C	
			BL=400 mm	25.0		14.62	F-C	
		C40 MPa	Ø10 mm GFRP, BL=400 mm	2.88		19.86	F-C	
		C50 MPa	BL=400 mm	13.85		15.37	F-C	
		Ø8 mm BFRP, C30 MPa	BL=500 mm	–		28.33	F-C	
			BL=600 mm	–		20.79	F-C	
		Ø8 mm GFRP, C30 MPa	BL=500 mm	–		24.19	Fr	
			BL=600 mm	–		22.48		
		Ø10 mm GFRP, C30 MPa	BL=500 mm	–		29.77		
			BL=600 mm	–		26.43		
		C40 MPa	Ø10 mm GFRP, BL=500 mm	–		32.81		
		C50 MPa	BL=500 mm	–		29.8		

Table 3 (continued)

Authors	Method and filling		Specimen designation	%P_u	Δy (mm)	Δu (mm)	Failure Mode	$\mu_{\Delta u}=\delta u/\delta y$
Hong and Park [116]	prestress levels of CFRP-NSM plate -with and without transverse grooves (TGs)		1 plate	42	13.3	50	F–C	
			1 plate, Prestressing force 10%	73	12.4	62.1		
			1 plate, Prestressing force 20%	79	12.1	52.8		
			1 plate, Prestressing force 30%	85	12.7	59.0		
			1 plate, Prestressing force 50%	85.6	13.7	49.6		
			1 plate, Prestressing force 20%+TGs	91.6	12.9	43.8		
			1 plate, Prestressing force 50%+TGs	96.1	14.2	46.7		
Sharaky et al. [117]	NSM FRP bars and MBRACE ADHESIVE HT (BASF)		1bar CFRP, d=8mm	55.3		31.7	S-Es	
			2bar CFRP, d=8mm	66.3		20.3	CCs	
			1 bars GFRP, d=8mm	62.6		22.0	Fr+Es	
			2 bars GFRP, d=8mm	41.2		59.7	F–C	
			1bar GFRP, d=12mm	50.3		35.3	S-Es	
	NSM FRP bars and POLYFIXER EP epoxy		2 bars CFRP, d=8mm	59.4		42.4	CCs	
			2 bars GFRP, d=8mm	56.3		42.3	S-Es+F–C	
Abdallah et al. [118]	SNSM-2∅6 CFRP rods	Resin Filling	Strengthening length/beam length=0.94	59	15.5	50.4	F–C	3.25
			Strengthening length/beam length=0.65	46	15.5	22.9	Peelingoff	1.48
		Mortar Filling	Strengthening length/beam length=0.94	45.6	15.7	38.2	S-Es	2.43
			Strengthening length/beam length=0.56	29.3	15.8	16.2	S-Es	1.03
		Resin Filling	Strengthening length/beam length=0.94	41.1	13.6	40.4	F–C	2.97
El-Gamal et al. [119]	2∅12 tension steel NSM		1∅10 CFRP bar	73	11	22	F	
			2∅10 CFRP bars	133	11	26		
			1∅10 GFRP bar	55	9	61	S-Cs	
			2∅10 GFRP bars	103	11	54	Fr	
	NSM and EB		1∅10 CFRP bar+1∅10 CFRP sheet	116	12	24		
			1∅10 GFRP bar+1∅10 CFRP sheet	87	11	22		
	4∅12 tension steel NSM		1 CFRP bar	31	10.5	28	F	
			2 CFRP bars	55	14	25		
Almusallam et al. [120]	2∅10 steel main tension bars		1∅10 steel NSM bar	3		37.14	S-Cs	7.27
			1∅14 steel NSM bar	41.9		39.51		6.31
			1∅10 GFRP NSM bar	19		38.75	Fr	7.57
	1∅10 steel main tension bars		2∅10 steel NSM bar	12.8		41.66	S-Cs	7.44
			2∅14 steel NSM bar	94.9		32.18		4.08
			2∅10 GFRP NSM bar	26.2		43.91	Fr	8.53

Table 3 (continued)

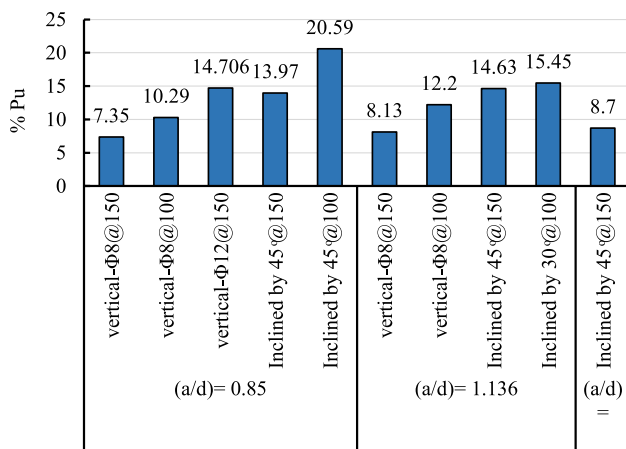| Authors	Method and filling	Specimen designation	% P_u	Δy (mm)	Δu (mm)	Failure Mode	$\mu_{\Delta u} = \delta u/\delta y$
Yu et al. [121]	NSM 7075 AA bars	1 Ø16 AA bars	35	11.20	50.09	IC	2.88
		2 Ø16 AA bars	87	10.03	49.06	CCs	2.85
		1Ø16 AA bars + CFRP U – jacket	50	11.04	61.80	S-Cs	5.60
		2 Ø16 AA bars + CFRP U – jacket	99	10.35	47.21	CCs + jacket rupture	3.82
Imjai et al. [122]	post-tension metal strapping (PTMS) and side-NSM (SNSM) FRP bars	PTMS	-		10.4	S-Cs	
		SNSM-CFRP bars at the compression side	-		11.0	S-Cs	
		SNSM-CFRP bars at tension side	-		10.5	S-Cs	
		Precracked + PTMS confinement	7		22.0	F-C	1.66
		Precracked + SNSM at top side	3		34.2	F-C	2.72
		Precracked + SNSM at bottom side	55.3		33.7	F-C	2.11
Deng et al. [123]	CFRP-NSM for ultra-high performance (UHPC) prestressed concrete prisms (CFRP-PCPs)	BL = 2200 mm + 0% Prestress CFRP	59.9		39.2	S-Cs	4.36
		BL = 1000 mm + 0% Prestress CFRP	7		80.08	F	–
		BL = 1400mm + 30% Prestress CFRP-UHPC	45.8		75.22	S-Es	–
		BL = 1800mm + 30% Prestress CFRP-UHPC	56.6		41.43	S-Cs	–
		BL = 2200 mm + 30% Prestress CFRP- UHPC	67.9		36.33	S-Cs	3.54
		BL = 2200 mm + 30% Prestress CFRP- Epoxy resin mortar prism	51.8		32.74	S-Es	–
		BL = 2200 mm, 50% Prestress CFRP- UHPC	55.9		33.5	S-Cs	2.65
Ebead and El-Sherif [114]	FRCM-NSM, 0.5% reinforcement ratio	(PBO)	57.1		28.1	SF	5.73
		CFRP-FRCM	48.4		16.1		3.21
		GFRP-FRCM	31.4		22.9	Fr	5.56
	FRCM-NSM, 1.27% reinforcement ratio	PBO-FRCM	83.5		26.2	SF	3.6
		CFRP-FRCM	84.3		17.5		2.45
		GFRP-FRCM	70.4		21.0	Fr	2.87
Shabana et al. [124]	2Ø10 CFRP-NSM bars fully and partially 90° end-hooked	1-fully bonded straight bar	56.6	12.7	28	CCs	2.2
		2-fully bonded straight bars	57.3	14.94	15.6	CCs	1.04
		2-fully bonded end-anchored bars	97.9	13.8	20.8	CCs	1.51
		2 partially bonded end-anchored bars 700 mm un-BL	96.6	13.6	25.3	CCs	1.86
		900 mm un-BL	76.2	12.2	20.2	SH	1.66
Attia et al. [125]	(GFRP) or steel -NSM, and U-jacket	3 layers GFRP	22		20.2	F	3.59
		60 mm width of GFRP, folded into 3 layers	19		18.1	F	2.98
		steel plate of 4 mm thickness	37		12.7	F	2.78
		recovering the U- section with steel fiber	14		14.4	F	2.85
		recovering the U- section with 3 strips of GFRP	28		18.6	F	2.93

Fig. 4 The % Pu of the beams with a shear span to the effective depth (a/d) ratio [112]
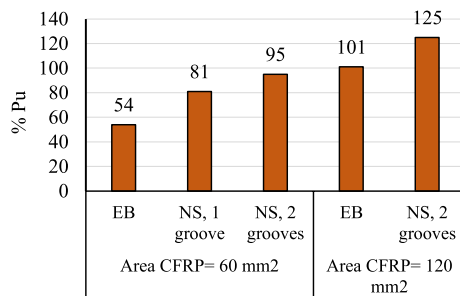

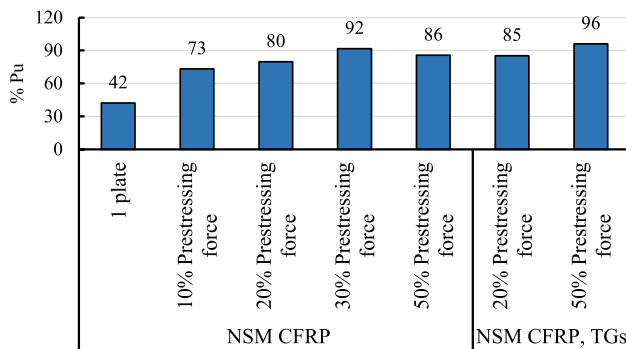**Fig. 5** The % P_u in RC beams strengthening by NSM and EBR techniques [113]

Fig. 6 The effect of prestress levels on % P_u of the beams strengthened with NSM-CFRP [116]
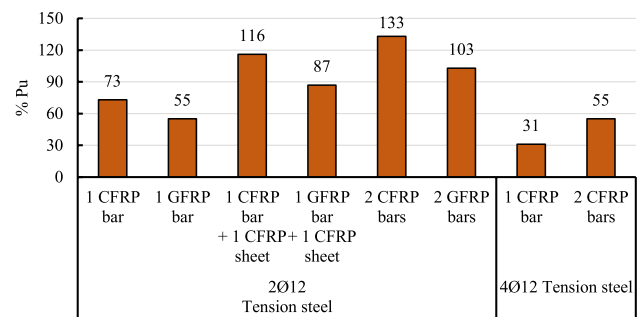

Fig. 7 The % P_u by increasing the amount of the FRP strengthening material [119]
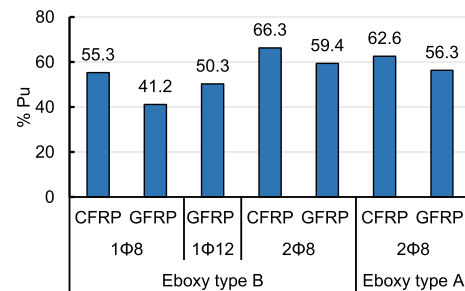
Fig. 8 The % P_u by increasing the number of NSM-CFRP bars and NSM-GFRP bars [117]

the prestressing levels but showed minimal effect on the ultimate load.

Zhu et al. [132] presented the results of the mechanical properties of RC beams strengthened with NSM basalt-FRP (BFRP) bars during and after exposure to high temperatures. They indicated that BFRP bars with epoxy resin matrix exhibit the best mechanical properties at ambient temperature. At the same time, the tensile strength decreased by approximately 20% during exposure to 200 °C. Alternatively, Gil et al. [133] examined the effect of post-tensioning strengthening using BFRP laminates using NSM-BFRP with no prestressing and NSM BFRP with prestressing presented by tensing the laminate within the concrete gaps. They found that the ultimate load increased by 63% compared to the CB, while similar deflections were achieved for both types.

Abdallah et al. [118] showed that side NSM (SNSM) strengthening could avoid specific non-conventional failure modes such as pullout or early debonding. Additionally, they observed that increasing the length of the CFRP bars (SL) improved not only the failure load of the beam but also the maximum CFRP strain (Fig. 9). Moreover, the CFRP rods located near the steel bars and embedded in resin were found to be more effective than those embedded in mortar or situated above the main tension steel. Furthermore, Zhu et al. [134] evaluated the performance of SNSM CFRP strengthening on large-scale RC beams. It was observed that, compared to CB, the flexural strength was improved by increasing the prestressing levels and reducing the CFRP spacing.

Yu et al. [121] showed that AA bars with high strength could enhance the beams' flexural stiffness but reduce their displacement ductility compared to un-strengthened ones (Fig. 10). Alternatively, Imjai et al. [122] reported that the capacity of pre-cracked post-tension
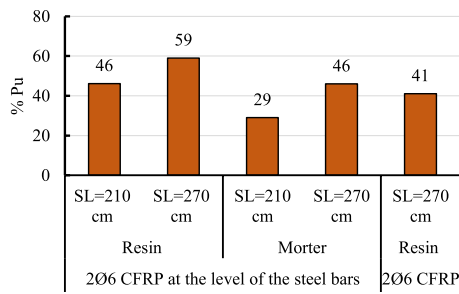
Fig. 9 The % P_u by increasing the length of the CFRP bars and changing the position [118]
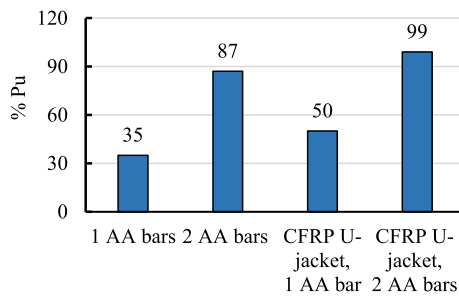

Fig. 10 The % Pu by increasing the number of the AA bars and CFRP U-jacket [121]

metal strapping (PTMS)- strengthened beam was only 8% higher than CB. Contrariwise, the SNSM increased the capability of the beam to 55% due to an additional flexural increase given by FRP bars, as shown in Table 3. In addition, Ibrahim et al. [135] demonstrated that different NSM-hybrid carbon/glass FRP strips showed a lower tensile strain for beams strengthened with two NSM-FRP strips than those with three NSM-FRP strips. On average, the flexural strengthening of RC beams with two NSM-FRP strips recorded strains up to 65%, corresponding to 96% for beams strengthened with three NSM-FRP strips.

Deng et al. [123] showed that prestressed NSM CFRP for ultra-high-performance concrete prisms (UHPC) was an effective and practical way to strengthen the RC beams. The ultimate load of the 30% prestressed beam with a 2000 mm bond length was 67.98% more than the CB. Moreover, Cruz et al. [136] conducted a study on beams strengthened with two different types of adhesives (stiff and flexible), considering the presence or absence of cracks in the concrete before the strengthening application. They found that when flexible adhesives were used instead of stiff adhesives, the load-carrying capacity values were slightly lower (roughly 19% less). Consequently, it also provided more ductile failure and higher residual load capacity (61% enhancement).

Mode of failure of the NSM system

Figure 11 shows the failure modes in this technique. It can be identified using the abbreviation (S, Cs, CCs, C, Es, Fr, and F) for steel yielding, concrete cover splitting, concrete cover separation, concrete crushing, epoxy-concrete debonding, epoxy splitting, FRP rupture, and FRP debonding, respectively.

Steel yielding followed by concrete cover splitting (S-Cs)

The splitting of the CC was caused by the growth of a major horizontal crack, which started from the presence of the shear fracture at the end of the FRP rods where a bending crack had existed [114, 116–120, 122, 127, 129, 134, 137]. This type of failure was expected when the stiffness of the NSM element was low (GFRP materials were an example [117, 138].

Concrete cover separation (CCs)

The CCs failure was a common failure mode of the NSM technique when the CFRP bars were used as a strengthening element [117, 139].

Steel yielding followed by splitting of the epoxy adhesive (S-Es)

First, the tension part of the concrete close to the middle span of the strengthened beam starts to crack. With increasing the applied load, the cracks propagate gradually toward the compressive side of the strengthened beam. When it reaches its ultimate load, the epoxy adhesive's cracking continues until a load breakage occurs [114, 117, 140]. The FPR rods were sheared off as the epoxy layer splintered into various pieces.

FRP debonding and concrete crushing (F–C)

At the start, vertical flexural cracks appear in the middle of the span. As further increases in load, these cracks grow wider; however, FRP reinforcement limited the crack width compared to the un-strengthened beam. Finally, failure occurred due to debonding between FRP strips at the strip-epoxy interface. This begins in the center of the span and is followed by the crushing of concrete [113, 117, 120, 130].
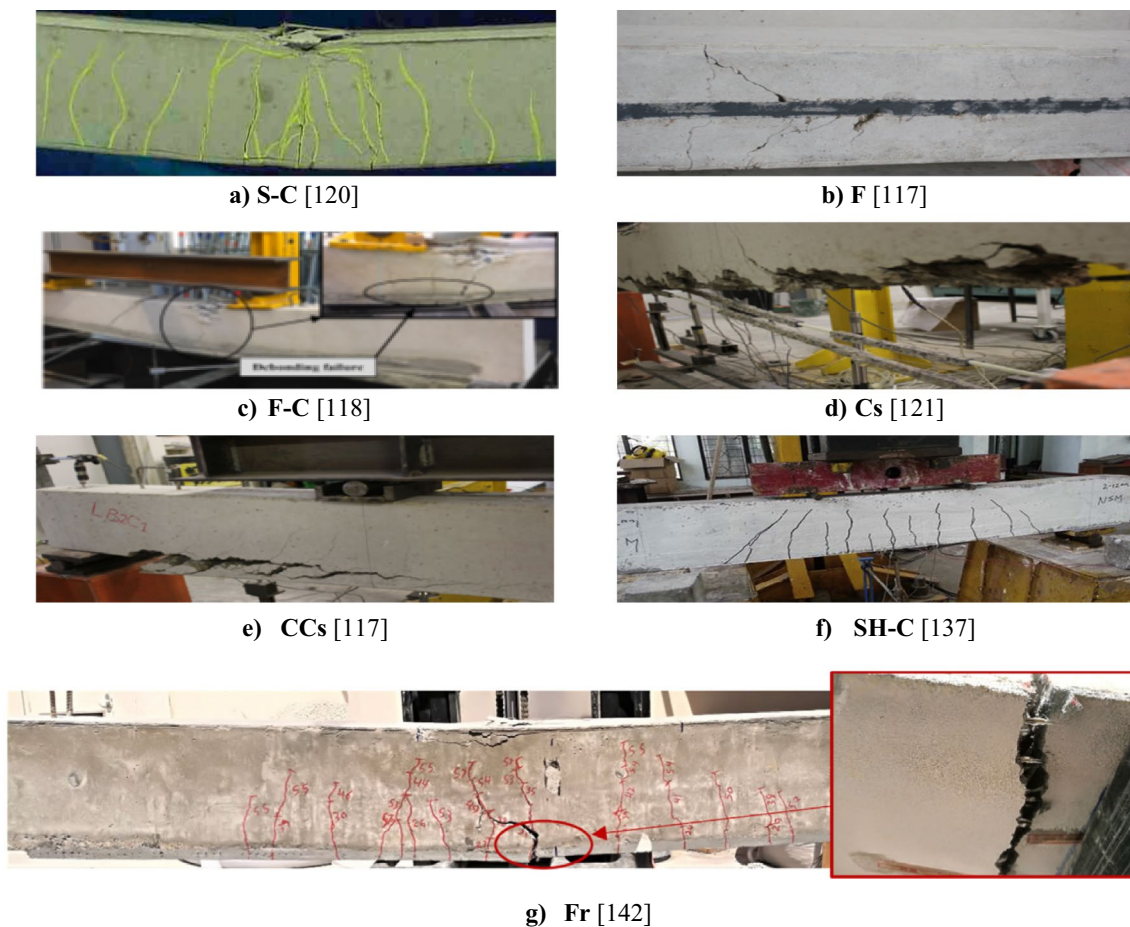
a) S-C [120]

b) F [117]

c) F-C [118]

d) Cs [121]

e) CCs [117]

f) SH-C [137]

g) Fr [142]

Fig. 11 Failure modes in NSM strengthening method

NSM FRP deboning (F)

In this mode, the failure is debonding at the interfacial zone between the adhesive and the fiber resulting in cracking and peeling of the adhesive [112, 119, 141].

NSM FRP rupture (Fr)

As the load increased, cracks in the concrete near the midspan expanded onto the surface of the epoxy adhesive, causing debonding of the epoxy-FRP interface, which led to the further splitting of the adhesive at the loaded end. Once the strengthened beam achieves its ultimate load, the FRP bars at that end rupture while the epoxy remains undamaged, and no occurrence of slippage at the free end [114, 115]. The higher prestress delays the separation of concrete covers, displaying a complete combination between the prestressed NSM CFRP plate and beam [124].

Shear failure (brittle failure)

In some cases, the reinforcement of specimens has led to the failure mode changing from ductile to brittle shear. This is not an ideal result. At the beginning of the process, there are cracks in the area close to the opening, but with FRP strips in place, these cracks cannot expand any further. The NSM strips continue resisting and supporting until they can no longer bear the load and eventually fail due to reaching their maximum shear capacity [127].

Strain response and ductility analysis of the NSM strengthening

The strengthening scheme has been proven effective in improving the ductility of concrete beams. Rather than brittle shear failure, strengthened beams experience more ductile flexural failure. Ductility relates to an object's capacity to remain in a state of inelastic deformation up

to failure without losing its load-carrying capacity. Experiments showed that as prestressing levels increase, the ductility decreases in RC beams strengthened with prestressed-NSM due to reducing usable strain with added pressure; however, it still causes an increase in cracking and yielding loads compared to samples without prestressing [116, 131, 134]. Ultimately, higher prestressing numbers decrease ductility index—for example, a decrease of 2.5% for beams of 10% prestressed and 35.6% for that of 50% prestressed with transverse grooves (TGs) was recorded [116]. As for prestressed CFRP, increasing prestressing gradually reduces ductility and prevents stiffness loss even after cracking [133]. Results showed that specimens with 30% of their ultimate force exhibited 66% less ductility than the CB [123]. Even after cracking of FRP, post-tensioned beams had a maximum 18% reduction in their effective stiffness, which is an excellent performance compared to CB.

Al-Issawi et al. [112] observed that the maximum deflection increased by about 57%, 34%, and 39% for shear spans/depth ratios of 0.85, 1.136, and 1.42, respectively, when reinforced with inclined bars. The RC beams strengthened by NSM and inclined by 90° had more strength and rigidity than those angled at 45°. The ductility of all the beams decreased compared to the un-strengthened concrete beams, but the beam with short side NSM bars with a 45° end anchorage had a noticeable amount of ductility [138]. Gopinath et al. [137] noticed that while the size of the groove and diameter of the BFRP bar can affect the steel bar's capacity to take the strain, the strain at maximum load remains almost similar for BFRP. Al-Mahmoud et al. [6] found that no significant decrease in deflection at ultimate load occurred for beams supplemented with 300 cm of CFRP rods; however, it led to an increase of 15 mm in the deflection after using 30 cm of extra anchorage length. Rasheed et al. [129] reported a ductility ratio of 90% in NSM strengthening techniques and an effective strain ratio of 0.88, mainly due to concrete crushing (FRP strain at failure = 0.015). The decrease in the ductile values of beams is inferred to be brought on by supplementing them with an insufficient length (210 cm), resulting in unconventional failure modes such as peeling off or early debonding failure [118]. When FRP area and stiffness increase, the beams' strain reduces, and subsequent deflection also decreases [117]. However, if the stiffness ratio goes beyond 1.25, the failure mode changes from concrete cover separation to concrete-epoxy or strip-epoxy interfaces; thus, overly-high stiffness has little to no effect. The best way to enhance the load-bearing capacity when stiffness crosses this level is by using an anchoring system [139]. The specimens anchorage with a CFRP U-jacket in the NSM method using AA bars in RC beams experienced a 94% and 34% increase in displacement ductility compared to the strengthened beams without U- jacket [121].

Parameters affecting the flexural property of NSM-strengthened beams

Type of NSM FRP material

The experimental results showed that beams reinforced with CFRP bars achieved loads between 155.3 and 166.3%, higher than those bolstered by GFRP bars (141.2–159.4%). Furthermore, increasing the area of GFRP bars had a more significant impact on the maximum load than CFRP bars [117]. Though they held more weight, CFRP-strengthened beams exhibited more brittle behavior [119]. The flexural performance of the strengthened beams increased by over 35% when using the NSM AA system [121]. Therefore, compared to beams reinforced with GFRP reinforcement, NSM-CFRP-bolstered beams produced better results with greater ultimate strength but poorer resistance to mid-span deflection.

The amount of NSM FRP

With the addition of NSM bars, Kotynia [126] revealed that the bond strain of a single CFRP strip surpasses that of double strips in lower steel percentage beams. Furthermore, the enhancement of post-tensioned NSM reinforcement to RC beams increased as additional bars were added. As the number of GFRP bars increases from one to two, the maximum measured crack width decreases by about 8% and 28%, respectively, compared to the REF beam [119]. However, when high reinforcement area was used, flexural capacity and pre-yield stiffness increased significantly, although deflection and energy ductility were severely affected [117, 120, 137]. Codes of practice limit the total tension steel ratio to prevent sudden compression failure. In particular, placing two CFRP strips in a single groove over attaching them increases the ultimate load between 19 and 74.5% [143]. Implementing NSM-CFRP strips distributed across two grooves instead of one can result in fewer crack widths and an increased ultimate load [113]. The hybrid method of NSM and EB beams displays lower capacities than the NSM beams with two bars [119].

The NSM bonded length

The effectiveness of CFRP plates in concrete repair and strengthening can be improved by increasing its length [6]. It was found that when the CFRP rods were extended by 60 cm, this prevented a non-conventional failure mode (peeling off) or delayed debonding failure, thus improving the efficiency as a reinforcing material [118]. Additionally, another research team noted that when bond lengths between FRP bars and strips increased, while the clear distance decreased, the ultimate strength and ductility increased [144]. This

supports the claim that short CFRP lengths can affect its repair and strengthen effectiveness. The beam capacity and NSM efficiency increased as the bond length became critical. Afterward, the increase rate became trivial with further increase in the bond length [6, 139, 144, 145].

The positioning of the NSM bars

When the NSM bars were arranged inclinedly, the load-carrying capacity increased by 9.33% compared to beams strengthened with only vertical bars [112]. However, there was a slight reduction in both the yield and the ultimate load-carrying capacities of the beam strengthened by CFRP upper the main tension steel. This is because the CFRP rods cause additional tensile stress above the level of steel bars, thereby decreasing the system's effective moment arm within the beam's cross-section [118].

Spacing between NSM bars

Longitudinal CFRP spacing reduction increased ultimate load and yield load in non-prestressed strengthened beams [112]. By decreasing the distance between NSM bars from 150 to 100 mm, the load capability increased by around 5.8% [112]. Moreover, increasing the GFRP bar size from 6 to 10 mm, and decreasing the spacing from 160 to 120 mm, will also result in a slight increase in loading capacity (less than 5%) [127]. Also, enhancing the area below the lateral neutral axis of the tested beam with SNSM improved the flexural capacity of this strengthened beam as CFRP strip spacing decreased [134].

NSM Bar diameter

Changing the diameter of vertical strengthening bars from 8 to 12 mm increased the load-carrying capacity by 6.85% [112]. This rise was even higher when NSM-CFRP bars increased by 13.12%, with a jump to 21.95% in maximum load capacity at the same failure mode. With a 50% increase in the diameter of NSM GFRP bars, the specimens experienced a 75.2% increase in failure load and experienced the same type of failure [12].

Anchorage systems

The beams reinforced with prestressed NSM-CFRP plates suddenly failed. Thus, the utilization of prestressed NSM-CFRP plates in field applications can be improved by preventing the issue of end anchoring. This could be done by clamping the mechanical anchorages at the ends of the plates and at the two ends of the NSM FRP bars to prevent separation of the concrete cover. Wrapping the FRP bars with a U-shaped fire protection board could be another measure to ensure that anchorage is maintained when exposed to high temperatures [132]. With these mechanical anchorages, it was found that the overall load-carrying capacity of the beams increased by 6–12% [121].

Epoxy

Sharaky et al. [117] conducted experimental work involving two types of epoxy resin (A and B). Type A, MBRACE ADHESIVE HT (BASF), consisted of primer and epoxy paste, while type B was POLYFIXER EP (ROBERLO). Comparing the average properties between the two resins, type A had a modulus of elasticity of 5761 MPa, compressive strength of 70.2 MPa, and tensile strength of 18.9 MPa. In contrast, type B had 8000 MPa, 95.5 MPa, and 23 MPa, respectively. The results indicated only a slight impact on the yielding and ultimate loads due to the choice of epoxy type because stability was governed by concrete cover separation (Fig. 8). Interestingly when comparing post-tensioned NSM strengthening with mortar filler versus the use of flexible adhesive, it was found that adhesive improved strengthening by 16% on uncracked series and 28% on cracked beams in comparison to mortar filler [136]. Moreover, after the maximum load-carrying capacity of the adhesive, CFRP continued to contribute, resulting in a post-failure residual load capacity of about 40% higher than achieved with steel reinforcement [136].

Beams strengthened with combined NSM technique and external FRP bonding

A combined NSM technique and external FRP bonding were developed as a new strengthening system to make reinforcing simpler and more accessible. Ferrier et al. [103] used 16 specimens with three types of reinforcement, composite fiber cement internally reinforced with CFRP or GFRP rods (CFCIR–CFRP or CFCIR–GFRP), NSM CFRP bars, and EB-CFRP plate in four-point bending load tests. According to the results, FRP reinforcement was found to limit both the crack opening and crack effects. Additionally, the new EB reinforcement system improved the mechanical properties of the RC beams at both service and failure levels by increasing bearing loads by 63%. Moreover, the study performed by El-Sherif et al. [142] showed that the hybrid near-surface embedded/externally bonded (NSE/EB) and FRCM could strengthen the RC beams. The increase in load capacity due to this strengthening scheme ranged from 24.8 to 109%. The test parameters variation led to different failure modes (plate-end delamination for beams strengthened with PBO-FRCM and fabric rupture for beams with GFRP-FRCM strengthening). The ductility decreased for specimens with low reinforcement ratios, while the post-crack

stiffness increased by 78%, 23%, and 56% for Carbon, PBO, and GFRP-FRCM reinforced beams.

Discussion

The beams strengthened with EB strengthening without end anchorage experienced load efficiency lower or higher than those with U- a wrapping sheet and end anchorage, depending on the failure mode. This means that the efficiency of the EB strengthened was not only affected by the end anchorage but also by the FRP area and EB shape due to the IC debonding failure [47–56, 58, 59, 61, 62, 68, 71–75, 83, 84, 86, 88–90, 92, 95, 97, 107, 146, 147]. The increase in EB area had the most significant effect on the beam capacity among all the factors affecting the EB strengthening. Conversely, the beams strengthened with NSM reinforcement without end anchorage experienced lower or higher load efficiency than those with end anchorage, depending mainly on the failure mode. The efficiency of the NSM strengthening was significantly affected by the end anchorage when the failure mode was CCs, while the end anchorage effect was trivial for beams that failed with bar rupture or Cs failures. Conversely, slight effects of FRP area were noticed for beams strengthened with NSM bars due to the CCs and Cs failure modes while using FRP strips was more efficient than the bars [13, 115–122, 124, 130, 134, 142, 148].

Table 4 shows the load efficiency of EB and NSM for the same beam dimensions and internal reinforcement. The table showed that the type of strengthening element greatly affected the EB and NSM efficiency. Abdallah et al. [5] found that the NSM recorded higher load efficiency than the EB one, although the NSM element had lower axial stiffness than the EB one. Khalifa [113] illustrated that with the same axial stiffness, the EB technique showed higher load efficiency than the NSM one. Rasheed et al. [129] mentioned that the failure mode significantly affects both EB and NSM techniques' efficiency.

Challenges and future research needs

Using fiber-reinforced polymer composite materials is a pretty option because it offers many advantages over the standard steel plate bonding technique, including a high strength/weight ratio, high corrosion resistance, and suppleness with the architectural uses [46]. Several researchers recommended using assorted end anchorage systems to avoid such a sudden premature debonding failure and ensure that strengthened members will develop their total flexural capacity. However, the high cost and manufacturing complexities of FRPs have made them impractical for use in civil applications, as noted by Wittocx et al. [149] and Mash

et al. [150]. This led to investigating whether repairing an existing structure is more environmentally and economically advantageous than constructing a new one [151]. The material prices will be roughly 16–17 times more when a comparable portion of CFRP was used in place of a standard steel plate, while for AFRP, the cost difference was almost eight times larger [152]. CFRP and GFRP are more expensive than AFRP. The cost of FRP components increased by prerequisite for particularly unique operational procedures [152]. Furthermore, GFRP was considered an excellent insulation and low-cost strengthening material [153]. Attributable to low price and intermediate mechanical properties, one of the potential applications of basalt fiber is the suitable combination with other composite materials for lightweight structures. Moreover, it reduced the usage of CFRP and maintained its high mechanical properties [154]. Basalt fiber has been introduced as an alternative to mixing glass fiber with carbon fiber [154]. However, the cost of CFRP material was several times more than steel plates. The fact that 6.2 kg of CFRP could be used instead of 175 kg of steel could explain the advantages of FRP over steel plates [155]. Attia et al. [125] found that using the NSM system with the steel plate method for beam strengthening had the lowest cost. Additionally, it resulted in the highest increase in the maximum load compared to all the other techniques. The study also found that based on the lowest cost beam, every 1 kN increase in the maximum load required 0.4 dollars. For beams strengthened using GFRP, the NSM system with GFRP, U-section with steel fiber, and three perpendicular strips of GFRP, the cost increases were 49.3%, 5.3%, 28.4%, and 191.6%, respectively. Sun et al. [156] suggested that cost-effective and potentially highly durable fillers could achieve more significant strength than conventional NSM methods with epoxy filler. Moreover, the high-viscosity fillers could also be easily installed for those side/bottom applications.

Soon, challenging times with a sharp increase of these RC buildings requiring repair or replacement could be expected with increased construction and demolition waste and the need for new construction material. The production process of cement as an essential component to produce concrete and repair mortar uses approximately 12–15% of the total industrial energy demand. Consequently, it represented around 5–7% of the global CO_2 emissions from all industrial processes and fossil-fuel combustion [149]. As a result, new composite materials based on inorganic cementitious matrices have been developed. These materials have led to the proposal of various cement-based strengthening systems for RC structures, such as textile-reinforced concrete (TRC), textile-reinforced mortar (TRM), fiber-reinforced cementitious matrix (FRCM), and fiber-reinforced grout (FRG) [157]. Also, to resolve the issue of compromised load transfer caused by anchorages, cost-effective alternatives such as

Table 4 The loading efficiency of EB and NSM for the same beam dimensions and internal reinforcement

Author	Beam characteristics			Axial stiffness (kN)		$1 + \frac{E_f \times A_f}{E_s \times A_s}$
	Method	% P_u	Fracture mode	$E_s \times A_s$	$E_f \times A_f$	
Abdallah et al. [5]	EB-CFRP-Sheet-1100 g/m2 of 150 mm width, 0.66 mm thickness, and by length/beam length=0.7 and 0.65 in the hogging and sagging regions on the top and bottom surfaces	50	IC debonding	59,375	19,635	1.38
	2∅6 NSM-CFRP rods in both the hogging and sagging regions, by length/beam length=0.7 and 0.65 in the hogging and sagging regions on the top and bottom surfaces	63.2	steel yielding and debonding of CFRP bars	59,375	9322.5	1.16
Klifa [113]	4 EB-CFRP strips with a width of 25 mm, a thickness of 1.2 mm for each strip, and 74% of the beam's span length	125	debonding at strip-epoxy and epoxy–concrete interfaces and concrete crushing		19,800	1.44
	4 NSM-CFRP strips with a width of 25 mm, a thickness of 1.2 mm for each strip, and 74% of the beam's span length, were installed into two grooves (two strips in each groove by 25 mm depth and 15 mm width)	101	peeling off of CFRP strips with concrete cover	45,239	19,800	1.44
Ebead and El-Sherif [114]	PBO-FRCM EB by 150 mm wide and 10 mm deep (low reinforcement ratio)	72.1	delamination at FRCM plate end	31,416	3605	1.11
	Carbon-FRCM EB by 150 mm wide and 10 mm deep for (high reinforcement ratio) beam	33	FRCM delamination at mid-span	810,425	3807	1.04
	PBO-FRCM NSE embedded into 90 mm wide and 10 mm deep groove over the full loaded length of the beam (low reinforcement ratio)	57	FRCM delamination at mid-span	31,416	3605	1.11
	Carbon-FRCM NSE embedded into 90 mm wide and 10 mm deep groove over the full loaded length of the beam (high reinforcement ratio)	25	FRCM delamination at mid-span	80,425	3807	1.04
Rasheed et al. [129]	2 layers of EB-CFRP sheets 4570 mm long and 559 mm wide on the bottom face, then turned up on the sides by 152 mm high+ 16 CFRP strips as transverse reinforcement by 152 mm wide and1067 mm long strips wrapped on the section	51	crushing of concrete cover (brittle failure) delamination of the CFRP+ fiber rupture at mid-span	226,822	21,299	1.094
	2 NSM-CFRP strips in four longitudinal grooves by19 mm deep, 6 mm wide, and along the length of the beam+44 single CFRP strips as transverse reinforcement (one strip in each groove by19 mm deep and 3 mm wide and 457 mm height)	46.3	concrete crushing, cracks in epoxy surrounding the CFRP strips, no splitting	226,822	33,536	1.15

cement-based paste and ceramic tile adhesive could provide a similar load capacity as that of epoxy-based methods. Furthermore, these substitutes were less sensitive to environmental factors, such as UV light and freeze–thaw cycles, than epoxy-based methods [156].

Although several testing standards have been published, further standardization is still required to encompass a broader range of weather conditions, test durations, types of test samples, and qualifications for testing personnel. Additionally, it would be intriguing to examine and test some of the initial constructions that were reinforced or strengthened with FRP to assess their long-term performance. This investigation could provide more insight into the actual behavior of such structures under real-world application, service, and weather conditions. Furthermore, it is necessary to compare different types of fibers based on their capacity for increasing strength, environmental effects, and cost. Finally, as almost all the discussed research were related to practical job and the concern of the uncertainty was not involved in these reviewed practical works which should be taken into account in the future work as was discussed in [158]. Conversely, in this paper the reviewed researches were aimed also to discuss the effect of the parameters affecting EB and NSM strengthening techniques, but the effect of these parameters was checked by small number of specimens and the other governing factors were changed from one research to another. To solve this problem the future work should include a sensitivity analysis to show the influence of these parameters on the results [159, 160].

Conclusions

1. The NSM method requires minimal surface preparation and is relatively easy to install, making it a cost-effective solution. Conversely, the EB technique involves complex surface preparation, such as cleaning and roughening the surface and applying a bonding agent.
2. The CCs failure mode was more common than the interfacial debonding failure mode for the RC beam upgraded with NSM CFRP elements. In contrast, IC debonding was the most common failure mode for EB strengthening.
3. Adding FRP U-jacket and end-anchorage systems to the EB or the NSM elements enhanced the strengthened system's load-bearing capacity and displacement ductility. The end anchorage was more efficient for EB and NSM strengthening when the failure is plate end-peeling and CCS, respectively. In contrast, the end anchorage had trivial effects on the EB/NSM efficiency when the failure mode is IC, CS, or FRP rupture.
4. Although FRP composite materials had many advantages compared to metallic materials as strengthening

elements, their higher cost and manufacturing difficulties made them impractical for civil engineering applications.
5. The NSM reinforcement technique was more efficient than the EB strengthening method for strengthening RC beams in flexural, while the NSM CFRP strips experienced superior efficiency among all other NSM FRP shapes (round bars and square bars) due to its high perimeter-to-area ratio.

The review offered significant gaps that need to be studied in future work as follows:

1. Few experimental studies were performed on continuous RC beams and frames compared to those treated with simply supported RC beams. In the simply supported beams, the sagging moment region was strengthened with the FRP reinforcement, so studying the efficiency of FRP in strengthening the hogging moment regions is still limited.
2. The effect of U-shaped FRP jackets and other end anchorages of EB and NSM strengthening was experimentally studied, but a design method to capture their impact is essential.
3. The review showed that only a few experimental studies were performed under high temperatures for the beams strengthened with EB and NSM strengthening. Studying the effect of high temperatures and direct fire on the behavior of RC beams strengthened with NSM/EB elements is necessary.
4. The use of CFRP materials as EB/NSM material was common for beams internally reinforced with steel, while using GFRP or CFRP elements as EB/NSM strengthening elements is still limited for beams internally reinforced with GFRP bars.

Declarations

Conflict of interest The authors declare that there are no conflicts of interest.

Ethical approval The authors declare that they have not submitted the manuscript to any other journal for simultaneous consideration. The work is original and not published elsewhere.

Informed consent Formal consent is not required for this type of study.

References

1. ACI Committee 440 (2007) Aci 440R-07: Report on Fiber-Reinforced Polymer (FRP) Reinforcement for Concrete Structures. p 104

2. Rankovic S, Folic R, Mijalkovic M (2010) Effects of RC beams reinforcement using near surface mounted reinforced FRP composites. Facta Univ - Ser Archit Civ Eng 8:177–185. https://doi.org/10.2298/fuace1002177r

3. Parvin A, Syed Shah T (2016) Fiber reinforced polymer strengthening of structures by near-surface mounting method. Polymers 8:298. https://doi.org/10.3390/polym8080298

4. De Lorenzis L, Teng JG (2007) Near-surface mounted FRP reinforcement: an emerging technique for strengthening structures. Compos Part B Eng 38:119–143. https://doi.org/10.1016/j.compositesb.2006.08.003

5. Abdallah M, Al Mahmoud F, Khelil A, Mercier J (2021) Efficiency of EB CFRP composites for flexural strengthening of continuous RC beams: a comparative study with NSM CFRP rods. Structures 34:1567–1588. https://doi.org/10.1016/j.istruc.2021.08.073

6. Al-Mahmoud F, Castel A, François R, Tourneur C (2009) Strengthening of RC members with near-surface mounted CFRP rods. Compos Struct 91:138–147. https://doi.org/10.1016/j.compstruct.2009.04.040

7. Wang X, Lam CC, Iu VP (2020) Bond behaviour of steel-TRM composites for strengthening masonry elements: experimental testing and numerical modelling. Constr Build Mater 253:119157. https://doi.org/10.1016/j.conbuildmat.2020.119157

8. Oehlers DJ, Liu I, Seracino R (2007) A generic design approach for EB and NSM longitudinally plated RC beams. Constr Build Mater 21:697–708. https://doi.org/10.1016/j.conbuildmat.2006.06.018

9. Rahal KN, Rumaih HA (2011) Tests on reinforced concrete beams strengthened in shear using near surface mounted CFRP and steel bars. Eng Struct 33:53–62. https://doi.org/10.1016/j.engstruct.2010.09.017

10. Thongchom C, Lenwari A, Aboutaha RS (2020) Bond properties between carbon fibre-reinforced polymer plate and fire-damaged concrete. Int J Adhes Adhes 97:102485. https://doi.org/10.1016/j.ijadhadh.2019.102485

11. Baghi H, Barros JAO, Menkulasi F (2016) Shear strengthening of reinforced concrete beams with Hybrid Composite Plates (HCP) technique: experimental research and analytical model. Eng Struct 125:504–520. https://doi.org/10.1016/j.engstruct.2016.07.023

12. Sharaky IA, Torres L, Baena M, Miàs C (2013) An experimental study of different factors affecting the bond of NSM FRP bars in concrete. Compos Struct 99:350–365. https://doi.org/10.1016/j.compstruct.2012.12.014

13. Reda RM, Sharaky IA, Ghanem M, Seleem MH, Sallam HEM (2016) Flexural behavior of RC beams strengthened by NSM GFRP Bars having different end conditions. Compos Struct 147:131–142. https://doi.org/10.1016/j.compstruct.2016.03.018

14. Solahuddin BA, Yahaya FM (2023) A narrative review on strengthening of reinforced concrete beams using carbon fibre reinforced polymer composite material through experimental investigation and numerical modelling. Structures 52:666–710. https://doi.org/10.1016/j.istruc.2023.03.168

15. Parghi A, Alam MS (2018) A review on the application of sprayed-FRP composites for strengthening of concrete and masonry structures in the construction sector. Compos Struct 187:518–534. https://doi.org/10.1016/j.compstruct.2017.11.085

16. Nie X, Zhang S, Gao Z, Zeng Z (2022) A review on the behaviour of reinforced concrete beams with fibre-reinforced polymer-strengthened web openings. Adv Struct Eng 25:426–450. https://doi.org/10.1177/13694332211046344

17. Kirthiga R, Elavenil S (2022) A review on using inorganic binders in fiber reinforced polymer at different conditions to strengthen reinforced concrete beams. Constr Build Mater 352:129054. https://doi.org/10.1016/j.conbuildmat.2022.129054

18. Wang Q, Zhu H, Zhang B, Tong Y, Teng F, Su W (2020) Anchorage systems for reinforced concrete structures strengthened with fiber-reinforced polymer composites: state-of-the-art review. J Reinf Plast Compos 39:327–344. https://doi.org/10.1177/0731684420905010

19. Sanginabadi K, Yazdani A, Mostofinejad D, Czaderski C (2022) Bond behavior of FRP composites attached to concrete using EBROG method: a state-of-the-art review. Compos Struct 299:116060. https://doi.org/10.1016/j.compstruct.2022.116060

20. Frhaan WKM, Abu Bakar BH, Hilal N, Al-Hadithi AI (2021) CFRP for strengthening and repairing reinforced concrete: a review. Innov Infrastruct Solut 6:1–13. https://doi.org/10.1007/s41062-020-00417-5

21. Abid SR, Al-lami K (2018) Critical review of strength and durability of concrete beams externally bonded with FRP. Cogent Eng 5:1–27. https://doi.org/10.1080/23311916.2018.1525015

22. Pan B, Liu F, Zhuge Y, Zeng J-J, Liao J (2022) ECCs/UHP-FRCCs with and without FRP reinforcement for structural strengthening/repairing: a state-of-the-art review. Constr Build Mater 316:125824. https://doi.org/10.1016/j.conbuildmat.2021.125824

23. Al-Osta MA (2018) Exploitation of ultrahigh-performance fibre-reinforced concrete for the strengthening of concrete structural members. Adv Civ Eng 2018:1–12. https://doi.org/10.1155/2018/8678124

24. Ortiz JD, Khedmatgozar Dolati SS, Malla P, Nanni A, Mehrabi A (2023) FRP-reinforced/strengthened concrete: state-of-the-art review on durability and mechanical effects. Materials 16:1–30. https://doi.org/10.3390/ma16051990

25. Zhu Y, Zhang Y, Hussein HH, Chen G (2020) Flexural strengthening of reinforced concrete beams or slabs using ultra-high performance concrete (UHPC): a state of the art review. Eng Struct 205:110035. https://doi.org/10.1016/j.engstruct.2019.110035

26. Awani O, El-Maaddawy T, Ismail N (2017) Fabric-reinforced cementitious matrix: a promising strengthening technique for concrete structures. Constr Build Mater 132:94–111. https://doi.org/10.1016/j.conbuildmat.2016.11.125

27. Nwankwo CO, Mahachi J, Olukanni DO, Musonda I (2023) Natural fibres and biopolymers in FRP composites for strengthening concrete structures: a mixed review. Constr Build Mater 363:129661. https://doi.org/10.1016/j.conbuildmat.2022.129661

28. Pham TM, Hao H (2016) Review of concrete structures strengthened with frp against impact loading. Structures 7:59–70. https://doi.org/10.1016/j.istruc.2016.05.003

29. Apandi NM, Ma CK, Chin CL, Awang AZ, Omar W, Rashid ASA, Zailani WWA (2023) Preliminary pre-damaged level assessment for concrete structures: A review. Structures 54:1381–1390. https://doi.org/10.1016/j.istruc.2023.05.130

30. Ferrari VJ, De Hanai JB, De Souza RA (2013) Flexural strengthening of reinforcement concrete beams using high performance fiber reinforcement cement-based composite (HPFRCC) and carbon fiber reinforced polymers (CFRP). Constr Build Mater 48:485–498. https://doi.org/10.1016/j.conbuildmat.2013.07.026

31. Qeshta IMI, Shafigh P, Jumaat MZ (2016) Research progress on the flexural behaviour of externally bonded RC beams. Arch Civ Mech Eng 16:982–1003. https://doi.org/10.1016/j.acme.2016.07.002

32. Obaidat YT, Heyden S, Dahlblom O, Abu-Farsakh G, Abdel-Jawad Y (2011) Retrofitting of reinforced concrete beams using composite laminates. Constr Build Mater 25:591–597. https://doi.org/10.1016/j.conbuildmat.2010.06.082

33. Sanginabadi K, Yazdani A, Mostofinejad D, Czaderski C (2022) RC members externally strengthened with FRP composites by grooving methods including EBROG and EBRIG: a state-of-the-art review. Constr Build Mater 324:126662. https://doi.org/10.1016/j.conbuildmat.2022.126662

34. Koutas LN, Tetta Z, Bournas DA, Triantafillou TC (2019) Strengthening of concrete structures with textile reinforced mortars: state-of-the-art review. J Compos Constr 23:1–20. https://doi.org/10.1061/(asce)cc.1943-5614.0000882

35. Huang Y, Grünewald S, Schlangen E, Luković M (2022) Strengthening of concrete structures with ultra high performance fiber reinforced concrete (UHPFRC): a critical review. Constr Build Mater. https://doi.org/10.1016/j.conbuildmat.2022.127398

36. Bandara S, Wijesundara K, Rajeev P (2023) Ultra-high-performance fibre-reinforced concrete for rehabilitation and strengthening of concrete structures: a suitability assessment. Buildings. https://doi.org/10.3390/buildings13030614

37. Al-Saadi NTK, Mohammed A, Al-Mahaidi R, Sanjayan J (2019) A state-of-the-art review: Near-surface mounted FRP composites for reinforced concrete structures. Constr Build Mater 209:748–769. https://doi.org/10.1016/j.conbuildmat.2019.03.121

38. Kadhim MMA, Altaee MJ, Adheem AH, Chabuk A, Al-Ansari N (2021) Review on NSM CFRP strengthened RC concrete beams in shear. Adv Civ Eng. https://doi.org/10.1155/2021/1074010

39. Yu JG, Cheng L, Liu S, Fu B, Li B (2021) Inorganic adhesive based near-surface-mounted fibre reinforced polymer for strengthening of concrete structures: an overview. Structures 33:2099–2120. https://doi.org/10.1016/j.istruc.2021.04.017

40. Zhang SS, Yu T, Chen GM (2017) Reinforced concrete beams strengthened in flexure with near-surface mounted (NSM) CFRP strips: current status and research needs. Compos Part B Eng 131:30–42. https://doi.org/10.1016/j.compositesb.2017.07.072

41. Al-Saadi NTK, Mohammed A, Al-Mahaidi R, Sanjayan J (2019) Performance of NSM FRP embedded in concrete under monotonic and fatigue loads: state-of-the-art review. Aust J Struct Eng 20:89–114. https://doi.org/10.1080/13287982.2019.1605686

42. Jedrzejko MJ, Zhang SS, Ke Y, Fernando D, Nie XF (2023) Shear strengthening of RC beams with NSM FRP. I: review of strength models. Adv Struct Eng 26:564–586. https://doi.org/10.1177/13694332221125832

43. Effiong JU, Ede AN (2022) Experimental investigation on the strengthening of reinforced concrete beams using externally bonded and near-surface mounted natural fibre reinforced polymer composites—a review. Materials. https://doi.org/10.3390/ma15175848

44. Siddika A, Al MMA, Ferdous W, Alyousef R (2020) Performances, challenges and opportunities in strengthening reinforced concrete structures by using FRPs: a state-of-the-art review. Eng Fail Anal 111:104480. https://doi.org/10.1016/j.engfailanal.2020.104480

45. Aslam M, Shafigh P, Jumaat MZ, Shah SNR (2015) Strengthening of RC beams using prestressed fiber reinforced polymers: a review. Constr Build Mater 82:235–256. https://doi.org/10.1016/j.conbuildmat.2015.02.051

46. Naser MZ, Hawileh RA, Abdalla JA (2019) Fiber-reinforced polymer composites in strengthening reinforced concrete structures: a critical review. Eng Struct 198:109542. https://doi.org/10.1016/j.engstruct.2019.109542

47. Salama ASD, Hawileh RA, Abdalla JA (2019) Performance of externally strengthened RC beams with side-bonded CFRP sheets. Compos Struct 212:281–290. https://doi.org/10.1016/j.compstruct.2019.01.045

48. Chen C, Yang Y, Yu J, Yu J, Tan H, Sui L, Zhou Y (2020) Eco-friendly and mechanically reliable alternative to synthetic FRP in externally bonded strengthening of RC beams: natural FRP. Compos Struct 241:112081. https://doi.org/10.1016/j.compstruct.2020.112081

49. Huang L, Yan B, Yan L, Xu Q, Tan H, Kasal B (2016) Reinforced concrete beams strengthened with externally bonded natural flax FRP plates. Compos Part B Eng 91:569–578. https://doi.org/10.1016/j.compositesb.2016.02.014

50. Abdalla JA, Abu-Obeidah AR, Hawileh RA (2019) Use of aluminum alloy plates as externally bonded shear reinforcement for R/C beams. Procedia Struct Integr 17:403–410. https://doi.org/10.1016/j.prostr.2019.08.053

51. Rasheed HA, Abdalla J, Hawileh R, Al-Tamimi AK (2017) Flexural behavior of reinforced concrete beams strengthened with externally bonded aluminum alloy plates. Eng Struct 147:473–485. https://doi.org/10.1016/j.engstruct.2017.05.067

52. Hawileh RA, Nawaz W, Abdalla JA (2018) Flexural behavior of reinforced concrete beams externally strengthened with Hardwire Steel-Fiber sheets. Constr Build Mater 172:562–573. https://doi.org/10.1016/j.conbuildmat.2018.03.225

53. Hawileh RA, Rasheed HA, Abdalla JA, Al-Tamimi AK (2014) Behavior of reinforced concrete beams strengthened with externally bonded hybrid fiber reinforced polymer systems. Mater Des 53:972–982. https://doi.org/10.1016/j.matdes.2013.07.087

54. Zhou CY, Yu YN, Xie EL (2020) Strengthening RC beams using externally bonded CFRP sheets with end self-locking. Compos Struct 241:112070. https://doi.org/10.1016/j.compstruct.2020.112070

55. Hosen MA, Jumaat MZ, Alengaram UJ, Sulong NHR, Islam ABMS (2019) Structural performance of lightweight concrete beams strengthened with side-externally bonded reinforcement (S-EBR) technique using CFRP fabrics. Compos Part B Eng 176:107323. https://doi.org/10.1016/j.compositesb.2019.107323

56. Nader Tehrani B, Mostofinejad D, Hosseini SM (2019) Experimental and analytical study on flexural strengthening of RC beams via prestressed EBROG CFRP plates. Eng Struct. https://doi.org/10.1016/j.engstruct.2019.109395

57. Dong J, Wang Q, Guan Z (2013) Structural behaviour of RC beams with external flexural and flexural–shear strengthening by FRP sheets. Compos Part B Eng 44:604–612. https://doi.org/10.1016/j.compositesb.2012.02.018

58. Al-Tamimi AK, Hawileh R, Abdalla J, Rasheed HA (2011) Effects of ratio of cfrp plate length to shear span and end anchorage on flexural behavior of SCC RC beams. J Compos Constr 15:908–919. https://doi.org/10.1061/(asce)cc.1943-5614.0000221

59. Ahmed E, Sobuz HR, Sutan NM (2011) Flexural performance of CFRP strengthened RC beams with different degrees of strengthening schemes. Int J Phys Sci 6:2229–2238. https://doi.org/10.5897/IJPS11.304

60. El-Sayed AK, Al-Zaid RA, Al-Negheimish AI, Shuraim AB, Alhozaimy AM (2014) Long-term behavior of wide shallow RC beams strengthened with externally bonded CFRP plates. Constr

Build Mater 51:473–483. https://doi.org/10.1016/j.conbuildmat.2013.10.055

61. Yin J, Wu ZS (2003) Structural performances of short steel-fiber reinforced concrete beams with externally bonded FRP sheets. Constr Build Mater 17:463–470

62. Ali H, Assih J, Li A (2021) Flexural capacity of continuous reinforced concrete beams strengthened or repaired by CFRP/GFRP sheets. Int J Adhes Adhes 104:102759. https://doi.org/10.1016/j.ijadhadh.2020.102759

63. Shahinur S, Hasan M (2020) Natural fiber and synthetic fiber composites: comparison of properties, performance, cost and environmental benefits. Encycl Renew Sustain Mater. https://doi.org/10.1016/b978-0-12-803581-8.10994-4

64. Zhang S, Wu B (2019) Effects of salt solution on the mechanical behavior of concrete beams externally strengthened with AFRP. Constr Build Mater. https://doi.org/10.1016/j.conbuildmat.2019.117044

65. Zhou A, Qiu Q, Chow CL, Lau D (2020) Interfacial performance of aramid, basalt and carbon fiber reinforced polymer bonded concrete exposed to high temperature. Compos Part A Appl Sci Manuf 131:105802. https://doi.org/10.1016/j.compositesa.2020.105802

66. Deng ZC, Xiao R (2011) Flexural performance of RC beams strengthened with Prestressed AFRP sheets: Part II. Theoretical analysis. Adv FRP Compos Civ Eng - Proc 5th Int Conf FRP Compos Civ Eng CICE 2010 704–707. https://doi.org/10.1007/978-3-642-17487-2_155

67. Dhand V, Mittal G, Rhee KY, Park SJ, Hui D (2015) A short review on basalt fiber reinforced polymer composites. Compos Part B Eng 73:166–180. https://doi.org/10.1016/j.compositesb.2014.12.011

68. Sim J, Park C, Moon DY (2005) Characteristics of basalt fiber as a strengthening material for concrete structures. Compos Part B Eng 36:504–512. https://doi.org/10.1016/j.compositesb.2005.02.002

69. Stephen I, Hughes E, Das S (2020) Reinforced concrete beams strengthened with basalt fibre fabric: a parametric study. Structures 27:309–318. https://doi.org/10.1016/j.istruc.2020.05.008

70. Hosny A, Shaheen H, Abdelrahman A, Elafandy T (2006) Performance of reinforced concrete beams strengthened by hybrid FRP laminates. Cem Concr Compos 28:906–913. https://doi.org/10.1016/j.cemconcomp.2006.07.016

71. Attari N, Amziane S, Chemrouk M (2012) Flexural strengthening of concrete beams using CFRP, GFRP and hybrid FRP sheets. Constr Build Mater 37:746–757. https://doi.org/10.1016/j.conbuildmat.2012.07.052

72. Choobbor SS, Hawileh RA, Abu-Obeidah A, Abdalla JA (2019) Performance of hybrid carbon and basalt FRP sheets in strengthening concrete beams in flexure. Compos Struct 227:111337. https://doi.org/10.1016/j.compstruct.2019.111337

73. Nayak AN, Kumari A, Swain RB (2018) Strengthening of RC beams using externally bonded fibre reinforced polymer composites. Structures 14:137–152. https://doi.org/10.1016/j.istruc.2018.03.004

74. Mostofinejad D, Shameli SM (2013) Externally bonded reinforcement in grooves (EBRIG) technique to postpone debonding of FRP sheets in strengthened concrete beams. Constr Build Mater 38:751–758. https://doi.org/10.1016/j.conbuildmat.2012.09.030

75. Moradi E, Naderpour H, Kheyroddin A (2020) An experimental approach for shear strengthening of RC beams using a proposed technique by embedded through-section FRP sheets. Compos Struct 238:111988. https://doi.org/10.1016/j.compstruct.2020.111988

76. Joshi SV, Drzal LT, Mohanty AK, Arora S (2004) Are natural fiber composites environmentally superior to glass fiber reinforced composites? Compos Part A Appl Sci Manuf 35:371–376. https://doi.org/10.1016/j.compositesa.2003.09.016

77. Yan L, Chouw N, Jayaraman K (2014) Flax fibre and its composites: a review. Compos Part B Eng 56:296–317. https://doi.org/10.1016/j.compositesb.2013.08.014

78. Wang W, Chouw N (2017) Behaviour of CFRC beams strengthened by FFRP laminates under static and impact loadings. Constr Build Mater 155:956–964. https://doi.org/10.1016/j.conbuildmat.2017.08.031

79. Li Y, Mai Y, Ye L (2000) Sisal fibre and its composites: a review of recent developments. Compos Sci Technol 60:2037–2055. https://doi.org/10.1016/S0266-3538(00)00101-9

80. Yinh S, Hussain Q, Joyklad P, Chaimahawan P, Rattanapitikon W, Limkatanyu S, Pimanmas A (2021) Strengthening effect of natural fiber reinforced polymer composites (NFRP) on concrete. Case Stud Constr Mater 15:e00653. https://doi.org/10.1016/j.cscm.2021.e00653

81. Hussain Q, Ruangrassamee A, Tangtermsirikul S, Joyklad P (2020) Behavior of concrete confined with epoxy bonded fiber ropes under axial load. Constr Build Mater 263:120093. https://doi.org/10.1016/j.conbuildmat.2020.120093

82. Ombres L (2015) Analysis of the bond between Fabric Reinforced Cementitious Mortar (FRCM) strengthening systems and concrete. Compos Part B Eng 69:418–426. https://doi.org/10.1016/j.compositesb.2014.10.027

83. Paschalis SA, Lampropoulos AP, Tsioulou O (2018) Experimental and numerical study of the performance of ultra high performance fiber reinforced concrete for the flexural strengthening of full scale reinforced concrete members. Constr Build Mater 186:351–366. https://doi.org/10.1016/j.conbuildmat.2018.07.123

84. Deng M, Ma F, Ye W, Li F (2018) Flexural behavior of reinforced concrete beams strengthened by HDC and RPC. Constr Build Mater 188:995–1006. https://doi.org/10.1016/j.conbuildmat.2018.08.124

85. Giese ACH, Giese DN, Dutra VFP, Da Silva Filho LCP (2021) Flexural behavior of reinforced concrete beams strengthened with textile reinforced mortar. J Build Eng. https://doi.org/10.1016/j.jobe.2020.101873

86. Alharthi YM, Emara M, Elamary AS, Sharaky IA (2021) Flexural response and load capacity of reinforced concrete beams strengthened with reinforced mortar layer. Eng Struct 245:112884. https://doi.org/10.1016/j.engstruct.2021.112884

87. Xing G, Wu T, Liu B, Huang H, Gu S (2010) Experimental investigation of reinforced concrete T-beams strengthened with steel wire mesh embedded in polymer mortar overlay. Adv Struct Eng 13:69–79

88. Qeshta IMI, Shafigh P, Jumaat MZ (2015) Flexural behaviour of RC beams strengthened with wire mesh-epoxy composite. Constr Build Mater 79:104–114. https://doi.org/10.1016/j.conbuildmat.2015.01.013

89. Douier K, Hawileh RA, Abdalla JA (2020) Effect of U-wrap anchors on the strength and ductility of externally bonded RC beams with mortar bonded GSM sheets. Procedia Struct Integr 28:986–993. https://doi.org/10.1016/j.prostr.2020.11.113

90. Abuodeh OR, Abdalla JA, Hawileh RA (2019) The flexural behavior of bolting and bonding aluminum alloy plates to RC beams. Procedia Struct Integr 17:395–402. https://doi.org/10.1016/j.prostr.2019.08.052

91. Wu ZM, Hu CH, Wu YF, Zheng JJ (2011) Improved hybrid bonding technique for attaching FRP to reinforced concrete beams. Mag Concr Res 63:861–869. https://doi.org/10.1680/macr.2011.63.11.861

92. Zhou Y, Gou M, Zhang F, Zhang S, Wang D (2013) Reinforced concrete beams strengthened with carbon fiber reinforced polymer by friction hybrid bond technique: experimental

investigation. Mater Des 50:130–139. https://doi.org/10.1016/j.matdes.2013.02.089

93. Zhang F, Gao L, Wu YF, Liu J (2021) Flexural design of reinforced concrete structures strengthened with hybrid bonded FRP. Compos Struct 269:113996. https://doi.org/10.1016/j.compstruct.2021.113996

94. Elsayed WE, Ebead UA, Neale KW (2009) Mechanically fastened frp-strengthened two-way concrete slabs with and without cutouts. J Compos Constr 13:198–207. https://doi.org/10.1061/(asce)cc.1943-5614.0000004

95. Ebead U (2011) Hybrid externally bonded/mechanically fastened fiber-reinforced polymer for rc beam strengthening. ACI Struct J 108:1–10. https://doi.org/10.14359/51683365

96. Hadhood A, Agamy MH, Abdelsalam MM, Mohamed HM, Aly El-Sayed T (2019) Shear strengthening of hybrid externally-bonded mechanically-fastened concrete beams using short CFRP strips: experiments and theoretical evaluation. Eng Struct 201:109795. https://doi.org/10.1016/j.engstruct.2019.109795

97. Ramesh B, Eswari S (2020) Structural response of GFRP strengthened hybrid fibre reinforced concrete beams. Mater Today Proc 33:463–469. https://doi.org/10.1016/j.matpr.2020.05.039

98. ACI Committee 440 (2008) ACI 440.2R-02-Guide for the design and construction of externally bonded frp systems for strengthening concrete structures. pp 1627–1633

99. Wroblewski L, Hristozov D, Sadeghian P (2016) Durability of bond between concrete beams and FRP composites made of flax and glass fibers. Constr Build Mater 126:800–811. https://doi.org/10.1016/j.conbuildmat.2016.09.095

100. Hanoon AN, Jaafar MS, Hejazi F, Aziz FNAA (2017) Strut-and-tie model for externally bonded CFRP-strengthened reinforced concrete deep beams based on particle swarm optimization algorithm: CFRP debonding and rupture. Constr Build Mater 147:428–447. https://doi.org/10.1016/j.conbuildmat.2017.04.094

101. Oller E, Pujol M, Marí A (2019) Contribution of externally bonded FRP shear reinforcement to the shear strength of RC beams. Compos Part B Eng 164:235–248. https://doi.org/10.1016/j.compositesb.2018.11.065

102. Wan B, Jiang C, Wu YF (2018) Effect of defects in externally bonded FRP reinforced concrete. Constr Build Mater 172:63–76. https://doi.org/10.1016/j.conbuildmat.2018.03.217

103. Ferrier E, Si Larbi A, Georgin JF, Ambroise J (2012) New hybrid cement-based composite material externally bonded to control RC beam cracking. Constr Build Mater 36:36–45. https://doi.org/10.1016/j.conbuildmat.2012.04.104

104. Razaqpur AG, Cameron R, Mostafa AAB (2020) Strengthening of RC beams with externally bonded and anchored thick CFRP laminate. Compos Struct 233:111574. https://doi.org/10.1016/j.compstruct.2019.111574

105. Xiong GJ, Yang JZ, Ji ZB (2004) Behavior of Reinforced Concrete Beams Strengthened with Externally Bonded Hybrid Carbon Fiber-Glass Fiber Sheets. J Compos Constr 8:275–278. https://doi.org/10.1061/(ASCE)1090-0268(2004)8:3(275)

106. Escrig C, Gil L, Bernat-Maso E (2017) Experimental comparison of reinforced concrete beams strengthened against bending with different types of cementitious-matrix composite materials. Constr Build Mater 137:317–329. https://doi.org/10.1016/j.conbuildmat.2017.01.106

107. Chen C, Yang Y, Zhou Y, Xue C, Chen X, Wu H, Sui L, Li X (2020) Comparative analysis of natural fiber reinforced polymer and carbon fiber reinforced polymer in strengthening of reinforced concrete beams. J Clean Prod 263:121572. https://doi.org/10.1016/j.jclepro.2020.121572

108. Panigrahi AK, Biswal KC, Barik MR (2014) Strengthening of shear deficient RC T-beams with externally bonded GFRP sheets.

Constr Build Mater 57:81–91. https://doi.org/10.1016/j.conbuildmat.2014.01.076

109. Sabzi J, Esfahani MR, Ozbakkaloglu T, Farahi B (2020) Effect of concrete strength and longitudinal reinforcement arrangement on the performance of reinforced concrete beams strengthened using EBR and EBROG methods. Eng Struct 205:110072. https://doi.org/10.1016/j.engstruct.2019.110072

110. Wang YC, Hsu K (2009) Design recommendations for the strengthening of reinforced concrete beams with externally bonded composite plates. Compos Struct 88:323–332. https://doi.org/10.1016/j.compstruct.2007.12.001

111. Toutanji HA, Gómez W (1997) Durability characteristics of concrete beams externally bonded with FRP composite sheets. Cem Concr Compos 19:351–358. https://doi.org/10.1016/S0958-9465(97)00028-0

112. Al-Issawi ASH, Kamonna HH (2020) Experimental study of RC deep beams strengthened by NSM steel bars. Mater Today Proc 20:540–547. https://doi.org/10.1016/j.matpr.2019.09.186

113. Khalifa AM (2016) Flexural performance of RC beams strengthened with near surface mounted CFRP strips. Alexandria Eng J 55:1497–1505. https://doi.org/10.1016/j.aej.2016.01.033

114. Ebead U, El-Sherif HE (2019) Near surface embedded-FRCM for flexural strengthening of reinforced concrete beams. Constr Build Mater 204:166–176. https://doi.org/10.1016/j.conbuildmat.2019.01.145

115. Zhang H, He L, Li G (2015) Bond failure performances between near-surface mounted FRP bars and concrete for flexural strengthening concrete structures. Eng Fail Anal 56:39–50. https://doi.org/10.1016/j.engfailanal.2015.04.018

116. Hong S, Park S-K (2016) Effect of prestress and transverse grooves on reinforced concrete beams prestressed with near-surface-mounted carbon fiber-reinforced polymer plates. Compos Part B Eng 91:640–650. https://doi.org/10.1016/j.compositesb.2016.01.018

117. Sharaky IA, Torres L, Comas J, Barris C (2014) Flexural response of reinforced concrete (RC) beams strengthened with near surface mounted (NSM) fibre reinforced polymer (FRP) bars. Compos Struct 109:8–22. https://doi.org/10.1016/j.compstruct.2013.10.051

118. Abdallah M, Al Mahmoud F, Boissière R, Khelil A, Mercier J (2020) Experimental study on strengthening of RC beams with Side Near Surface Mounted technique-CFRP bars. Compos Struct 234:111716. https://doi.org/10.1016/j.compstruct.2019.111716

119. El-Gamal SE, Al-Nuaimi A, Al-Saidy A, Al-Lawati A (2016) Efficiency of near surface mounted technique using fiber reinforced polymers for the flexural strengthening of RC beams. Constr Build Mater 118:52–62. https://doi.org/10.1016/j.conbuildmat.2016.04.152

120. Almusallam TH, Elsanadedy HM, Al-Salloum YA, Alsayed SH (2013) Experimental and numerical investigation for the flexural strengthening of RC beams using near-surface mounted steel or GFRP bars. Constr Build Mater 40:145–161. https://doi.org/10.1016/j.conbuildmat.2012.09.107

121. Yu X, Xing G, Chang Z (2020) Flexural behavior of reinforced concrete beams strengthened with near-surface mounted 7075 aluminum alloy bars. J Build Eng 31:101393. https://doi.org/10.1016/j.jobe.2020.101393

122. Imjai T, Setkit M, Garcia R, Figueiredo FP (2020) Strengthening of damaged low strength concrete beams using PTMS or NSM techniques. Case Stud Constr Mater 13:e00403. https://doi.org/10.1016/j.cscm.2020.e00403

123. Deng Y, Li Z, Zhang H, Corigliano A, Lam ACC, Hansapinyo C, Yan Z (2021) Experimental and analytical investigation on flexural behaviour of RC beams strengthened with NSM CFRP

prestressed concrete prisms. Compos Struct 257:113385. https://doi.org/10.1016/j.compstruct.2020.113385

124. Shabana IS, Sharaky IA, Khalil A, Hadad HS, Arafa EM (2018) Flexural response analysis of passive and active near-surface-mounted joints: experimental and finite element analysis. Mater Struct 51:107. https://doi.org/10.1617/s11527-018-1232-x

125. Attia MM, Abdelsalam BA, Tobbala DE, Rageh BO (2023) Flexural behavior of strengthened concrete beams with multiple retrofitting systems. Case Stud Constr Mater 18:e01862. https://doi.org/10.1016/j.cscm.2023.e01862

126. Kotynia R (2012) Bond between FRP and concrete in reinforced concrete beams strengthened with near surface mounted and externally bonded reinforcement. Constr Build Mater 32:41–54. https://doi.org/10.1016/j.conbuildmat.2010.11.104

127. Sakar G, Hawileh RA, Naser MZ, Abdalla JA, Tanarslan M (2014) Nonlinear behavior of shear deficient RC beams strengthened with near surface mounted glass fiber reinforcement under cyclic loading. Mater Des 61:16–25. https://doi.org/10.1016/j.matdes.2014.04.064

128. Qin G, Huang P, Zhou H, Guo X, Zheng X (2016) Fatigue and durability behavior of RC beams strengthened with CFRP under hot-wet environment. Constr Build Mater 111:735–742. https://doi.org/10.1016/j.conbuildmat.2016.02.131

129. Rasheed HA, Harrison RR, Peterman RJ, Alkhrdaji T (2010) Ductile strengthening using externally bonded and near surface mounted composite systems. Compos Struct 92:2379–2390. https://doi.org/10.1016/j.compstruct.2010.03.009

130. Lee HY, Jung WT, Chung W (2017) Flexural strengthening of reinforced concrete beams with pre-stressed near surface mounted CFRP systems. Compos Struct 163:1–12. https://doi.org/10.1016/j.compstruct.2016.12.044

131. Kara IF, Ashour AF, Köroḷlu MA (2016) Flexural performance of reinforced concrete beams strengthened with prestressed near-surface-mounted FRP reinforcements. Compos Part B Eng 91:371–383. https://doi.org/10.1016/j.compositesb.2016.01.023

132. Zhu H, Wu G, Zhang L, Zhang J, Hui D (2014) Experimental study on the fire resistance of RC beams strengthened with near-surface-mounted high-Tg BFRP bars. Compos Part B Eng 60:680–687. https://doi.org/10.1016/j.compositesb.2014.01.011

133. Gil L, Bernat-Masó E, Escrig C (2019) Experimental and analytical flexural performances of reinforced concrete beams strengthened with post-tensioned near surface mounted basalt composite laminates. Compos Part B Eng 157:47–57. https://doi.org/10.1016/j.compositesb.2018.08.072

134. Zhu Z, Zhu E (2018) Flexural behavior of large-size RC beams strengthened with side near surface mounted (SNSM) CFRP strips. Compos Struct 201:178–192. https://doi.org/10.1016/j.compstruct.2018.06.031

135. Ibrahim M, Wakjira T, Ebead U (2020) Shear strengthening of reinforced concrete deep beams using near-surface mounted hybrid carbon/glass fibre reinforced polymer strips. Eng Struct 210:110412. https://doi.org/10.1016/j.engstruct.2020.110412

136. Cruz JR, Serêga S, Sena-Cruz J, Pereira E, Kwiecień A, Zając B (2020) Flexural behaviour of NSM CFRP laminate strip systems in concrete using stiff and flexible adhesives. Compos Part B Eng 195:108042. https://doi.org/10.1016/j.compositesb.2020.108042

137. Gopinath S, Murthy AR, Patrawala H (2016) Near surface mounted strengthening of RC beams using basalt fiber reinforced polymer bars. Constr Build Mater 111:1–8. https://doi.org/10.1016/j.conbuildmat.2016.02.046

138. Sharaky IA, Reda RM, Ghanem M, Seleem MH, Sallam HEM (2017) Experimental and numerical study of RC beams strengthened with bottom and side NSM GFRP bars having different end conditions. Constr Build Mater 149:882–903. https://doi.org/10.1016/j.conbuildmat.2017.05.192

139. Sharaky IA, Baena M, Barris C, Sallam HEM, Torres L (2018) Effect of axial stiffness of NSM FRP reinforcement and concrete cover confinement on flexural behaviour of strengthened RC beams: Experimental and numerical study. Eng Struct 173:987–1001. https://doi.org/10.1016/j.engstruct.2018.07.062

140. Khorramian K, Sadeghian P (2019) Performance of high-modulus near-surface-mounted FRP laminates for strengthening of concrete columns. Compos Part B Eng 164:90–102. https://doi.org/10.1016/j.compositesb.2018.11.064

141. Foret G, Limam O (2008) Experimental and numerical analysis of RC two-way slabs strengthened with NSM CFRP rods. Constr Build Mater 22:2025–2030. https://doi.org/10.1016/j.conbuildmat.2007.07.027

142. El-Sherif H, Wakjira TG, Ebead U (2020) Flexural strengthening of reinforced concrete beams using hybrid near-surface embedded/externally bonded fabric-reinforced cementitious matrix. Constr Build Mater 238:117748. https://doi.org/10.1016/j.conbuildmat.2019.117748

143. Sharaky IA, Selmy SAI, El-Attar MM, Sallam HEM (2020) The influence of interaction between NSM and internal reinforcements on the structural behavior of upgrading RC beams. Compos Struct 234:111751. https://doi.org/10.1016/j.compstruct.2019.111751

144. Sharaky IA, Torres L, Sallam HEM (2015) Experimental and analytical investigation into the flexural performance of RC beams with partially and fully bonded NSM FRP bars/strips. Compos Struct 122:113–126. https://doi.org/10.1016/j.compstruct.2014.11.057

145. De Lorenzis L, Nanni A (2001) Characterization of FRP rods as near-surface mounted reinforcement. J Compos Constr 5:114

146. Liu C, Wang X, Shi J, Liu L, Wu Z (2021) Experimental study on the flexural behavior of RC beams strengthened with prestressed BFRP laminates. Eng Struct 233:111801. https://doi.org/10.1016/j.engstruct.2020.111801

147. Demir A, Ercan E, Demir DD (2018) Strengthening of reinforced concrete beams using external steel members. Steel Compos Struct 27:453–464. https://doi.org/10.12989/scs.2018.27.4.453

148. Al-Mahmoud F, Castel A, François R, Tourneur C (2010) RC beams strengthened with NSM CFRP rods and modeling of peeling-off failure. Compos Struct 92:1920–1930. https://doi.org/10.1016/j.compstruct.2010.01.002

149. Wittocx L, Buyle M, Audenaert A, Seuntjens O, Renne N, Craeye B (2022) Revamping corrosion damaged reinforced concrete balconies: life cycle assessment and life cycle cost of life-extending repair methods. J Build Eng 52:104436. https://doi.org/10.1016/j.jobe.2022.104436

150. Mash JA, Harries KA, Rogers C (2023) Repair of corroded steel bridge girder end regions using steel, concrete, UHPC and GFRP repair systems. J Constr Steel Res 207:107975. https://doi.org/10.1016/j.jcsr.2023.107975

151. Ferreira J, Duarte Pinheiro M, de Brito J (2015) Economic and environmental savings of structural buildings refurbishment with demolition and reconstruction: a Portuguese benchmarking. J Build Eng 3:114–126. https://doi.org/10.1016/j.jobe.2015.07.001

152. Chole A, Tembhurne A, Bawanthade A, Bhadade H, Ali Khan H, Kumar Shaw S (2023) Strengthening of reinforced concrete beams by using FRPs: an overview. Mater Today Proc. https://doi.org/10.1016/j.matpr.2023.05.149

153. Landesmann A, Seruti CA, Batista EDM (2015) Mechanical properties of glass fiber reinforced polymers members for structural applications. Mater Res 18:1372–1383. https://doi.org/10.1590/1516-1439.044615

154. Chen D, Sun G, Meng M, Jin X, Li Q (2019) Flexural performance and cost efficiency of carbon/basalt/glass hybrid FRP composite laminates. Thin-Walled Struct 142:516–531. https://doi.org/10.1016/j.tws.2019.03.056

155. Motavalli M, Czaderski C (2007) FRP composites for retrofitting of existing civil structures in Europe: State-of-the-art review. In: International conference of composites & polycon. american composites manufacturers Association, Tampa, FL USA, pp 17–19

156. Sun W, Lou T, Achintha M (2021) A novel strong and durable near-surface mounted (NSM) FRP method with cost-effective fillers. Compos Struct 255:112952. https://doi.org/10.1016/j.compstruct.2020.112952

157. Bencardino F, Condello A (2016) Eco-friendly external strengthening system for existing reinforced concrete beams. Compos Part B Eng 93:163–173. https://doi.org/10.1016/j.compositesb.2016.03.022

158. Shahri AA, Shan C, Larsson S (2022) A novel approach to uncertainty quantification in groundwater table modeling by automated predictive deep learning. Nat Resour Res 31:1351–1373. https://doi.org/10.1007/s11053-022-10051-w

159. Asheghi R, Hosseini SA, Saneie M, Shahri AA (2020) Updating the neural network sediment load models using different sensitivity analysis methods: a regional application. J Hydroinform 22:562–577. https://doi.org/10.2166/hydro.2020.098

160. Razavi S, Jakeman A, Saltelli A, Iooss B, Borgonovo E, Plischke E, Lo S, Iwanaga T, Becker W, Tarantola S, Guillaume JHA, Jakeman J, Gupta H, Melillo N, Rabitti G, Chabridon V, Duan Q, Sun X, Kucherenko S, Maier HR (2021) The future of sensitivity analysis : an essential discipline for systems modeling and policy support. Environ Modell Softw. https://doi.org/10.1016/j.envsoft.2020.104954